

U(1) problem and topological excitations on a lattice

S. Itoh, Y. Iwasaki, and T. Yoshié

Institute of Physics, University of Tsukuba, Ibaraki 305, Japan

(Received 20 February 1987)

We investigate in lattice QCD the U(1) problem that the η' meson (960 MeV) is much heavier than the π meson (140 MeV), taking Wilson fermions as quarks. We first derive the spectral representation of the quark propagator and investigate the Atiyah-Singer index theorem on a lattice. Then we calculate the η propagators as well as the π propagators for 10 configurations on an $8^3 \times 16$ lattice and show the following: The large splitting between the flavor-singlet pseudoscalar meson and the π meson is caused both by the existence of topologically nontrivial configurations and by the fact that the u and d bare-quark masses are very small. We further obtain that the mass of " η " $= (\bar{u}\gamma_5 u + d\gamma_5 d)/\sqrt{2}$ and the mass of $\eta_s = \bar{s}\gamma_5 s$ are both about 750 MeV. This is in accord with experiment, because if we assume the transition mass matrix between the two states is about 200 MeV, we obtain the correct masses for the η' and η mesons and the mixing angle $\phi = 10^\circ$ ($\eta' = \eta_1 \times \cos\phi + \eta_8 \sin\phi$). On the other hand there is no noticeable splitting between the ρ and ω mesons. We clarify the reason for the difference between the π - η splitting and the ρ - ω splitting. We point out that if the U(1) problem should be resolved both for Wilson quarks and for Kogut-Susskind quarks, the mechanisms would be completely different from each other. We also compare our results with the prediction of $1/N$ -expanded QCD.

I. INTRODUCTION

In continuum QCD, it is generally believed that an octet of pseudoscalar mesons (π , K , and η) would become massless Nambu-Goldstone bosons due to the spontaneous symmetry breaking of the SU(3)-octet axial symmetry in the limit of zero bare masses of u , d , and s quarks. In the real world, π , K , and η are only approximate Nambu-Goldstone bosons because the u , d , and s quarks possess small but nonzero bare masses. The U(1) current, the SU(3)-singlet axial-vector current, is also conserved naively in the limit of zero bare-quark masses. However, there is no conserved U(1) quantum number and the η' mass (960 MeV) is too heavy for the ninth approximate Nambu-Goldstone boson. This is the U(1) problem.¹

Actually the U(1) current has the triangle anomaly in quantum theory. 't Hooft² pointed out that topologically nontrivial gauge configurations such as instantons give the anomaly nonzero values and suggested that this is the resolution of the U(1) problem. However, there are no definite ways to compute hadron masses such as the η mass and the π mass quantitatively in continuum QCD. On the other hand, Witten³ and Veneziano⁴ derived in $1/N$ -expanded QCD the relation

$$\frac{f_\pi^2}{2N_f} \chi_t = m_{\eta'}^2 + m_\eta^2 - 2m_K^2, \quad (1.1)$$

where χ_t is the topological susceptibility, f_π is the pion decay constant ($f_\pi \simeq 90$ MeV), and N_f is the number of flavors. χ_t should be $(180 \text{ MeV})^4$ in order to give correctly the masses of K , η , and η' . Recently there have been several works computing the topological susceptibility on a lattice,⁵ although not yet conclusive. Furthermore, the relation itself is derived in the $1/N$ expansion and in the

chiral limit and therefore it is only an approximate relation for $N_c = 3$ and for a relatively large strange bare-quark mass m_s . Further discussion on $1/N$ -expanded QCD will be given in Sec. VIII.

The lattice formulation of QCD (Ref. 6) provides a definite way to compute hadronic physical quantities such as the π and η' masses by numerical methods. The purpose of this paper is to calculate directly the mass of the flavor-singlet pseudoscalar meson and to clarify the mechanism for the splitting between the flavor-singlet and -nonsinglet pseudoscalar mesons. A brief report of some results of the present paper has been given in Ref. 7. For earlier attempts see Ref. 8.

Let us discuss a little more about the U(1) problem. To account for the large mass of η' , 960 MeV, the mass of the pseudoscalar $(\bar{u}\gamma_5 u + \bar{d}\gamma_5 d)/\sqrt{2}$ should be heavier than the η meson (550 MeV) before the mixing with the $\eta_s = \bar{s}\gamma_5 s$. This is the U(1) problem in the world of two flavors. (See the discussion given in Sec. VII.) Thus we will deal with the pseudoscalar meson $(\bar{u}\gamma_5 u + \bar{d}\gamma_5 d)/\sqrt{2}$ with degenerate u and d bare masses and will call this particle the η meson for simplicity in this paper.

The organization of this paper is as follows. In Sec. II we introduce actions for quarks and gluons, in Sec. III we list several properties of the quark propagator including the spectral representation, and in Sec. IV we investigate the Atiyah-Singer index theorem on a lattice. We present the results of numerical calculations for the scalar and pseudoscalar densities in Sec. V and those for hadron propagators in Sec. VI. We describe in Sec. VII how to obtain the realistic values of the η and η' masses. Section VIII is devoted to discussion. In Appendix A we give the proofs of the properties given in Sec. III and in Appendix B we describe a slightly modified version of algorithm to solve the quark propagator.

II. ACTIONS FOR QUARKS AND GLUONS

We take Wilson fermions⁹ for quarks. (Some comments on Kogut-Susskind fermions¹⁰ will be given in Sec. VIII.) The action is given by

$$S_q = - \sum_{n,m} \bar{\psi}(n) D(n,m;K) \psi(m) , \quad (2.1)$$

with

$$D(n,m;K) = \delta_{nm} - K \sum_{\mu} [(1-\gamma_{\mu})U(n,\mu)\delta_{m,n+\hat{\mu}} + (1+\gamma_{\mu})U^{-1}(m,\mu)\delta_{n,m+\hat{\mu}}] . \quad (2.2)$$

We set $K_u = K_d = K$. One problem for Wilson fermions is the explicit chiral breaking even for flavor-nonsinglet axial-vector currents due to the Wilson term. In Ref. 11 we have given an argument that if we interpret the divergence of the axial-vector current as the definition of an interpolating field of π , we can derive the celebrated relations such as the Adler-Weisberger relation of current algebra. In Ref. 12 a stronger argument is given that the partially conserved axial-vector current can be defined nonperturbatively in the continuum limit. Anyway we believe that there are no fundamental problems for Wilson fermions concerning the chiral property in flavor-nonsinglet channels. In this paper we will investigate the chiral property in the flavor-singlet channel.

For gluons we take a renormalization-group- (RG-) improved SU(3) gauge action

$$S_g = \frac{1}{g^2} \left[c_0 \sum \text{Tr}(\text{simple plaquette loop}) + c_1 \sum \text{Tr}(1 \times 2 \text{ rectangular loop}) \right] , \quad (2.3)$$

with

$$c_1 = -0.331, \quad c_0 = 1 - 8c_1 . \quad (2.4)$$

The form of the action has been determined by a block-spin RG study¹³ and by an analysis of instantons on the lattice.^{14,15} In fact, in Ref. 14 we have first verified the existence of instantons by the following procedure. (i) By cooling gauge configurations which are randomly generated, we have found stable nontrivial configurations. These nontrivial configurations are the solutions for the lattice equation of motion. (ii) The values of the action of these nontrivial stable configurations are roughly integral multiples of $8\pi^2$. (iii) After proposing a definition for topological charge we have checked that the topological charge density is localized and that the relation

$$E \simeq 8\pi^2 |Q| \quad (2.5)$$

is satisfied. Here E is the value of the action and Q is the topological charge. (iv) The existence of stable (not quasistable) configurations for the cooling process depends on the form of gauge action. Further in Ref. 15 we have shown the following. (i) A parameter space, each point of which corresponds to a lattice action, is divided into two

regions: in one of them instantons are stable, while in the other they are not stable. (ii) The boundary between the two regions is close to the renormalized trajectory (RT) of a RG defined in Ref. 13. This fact is in accord with the idea that the RT represents effectively the long-distance behavior of any lattice action. Therefore the RG-improved action given by Eqs. (2.3) and (2.4) can take into account properly the effects of topological excitations such as instantons on a relatively small lattice at relatively small correlation length. Thus we take the RG-improved action for the study of the U(1) problem. We use periodic boundary conditions for both gauge fields and quark fields throughout this paper.

III. SPECTRAL REPRESENTATION OF D^{-1}

Let us consider the eigenvalue problems

$$D(K)\phi_i = \lambda_i \phi_i \quad (3.1)$$

and

$$\gamma_5 D(K)\chi_i = \mu_i \chi_i . \quad (3.2)$$

Then we can prove the following paragraphs (F1)–(F9) below. (The proofs of these facts are given in Appendix A.) The (F4) paragraph is not proven in the general case and therefore is a conjecture which has been checked numerically for various cases. Our main results are orthogonal relations (F6), and the spectral representation of D^{-1} (F7).

(F1). The eigenfunction ϕ_i is K independent and the eigenvalue λ_i is given by

$$\lambda_i = 1 - K/\rho_i , \quad (3.3)$$

where ρ_i is K independent. If λ_i is real, $\lambda_i = 0$ at $K = \rho_i$. Thus a real eigenvalue becomes a zero eigenvalue at some $K_c \equiv \rho_i$. In this case we call the eigenfunction a zero mode. On the other hand, μ_i and χ_i depend on K in complicated ways.

(F2). If λ_i is complex, λ_i^* is also an eigenvalue. We denote the corresponding eigenfunction by $\tilde{\phi}_i$:

$$D\tilde{\phi}_i = \lambda_i^* \tilde{\phi}_i . \quad (3.4)$$

(F3). If λ_i is an eigenvalue and ϕ_i is the corresponding eigenfunction:

$$D(K)\phi_i = \lambda_i \phi_i, \quad \lambda_i = 1 - K/\rho_i , \quad (3.5)$$

then

$$D(K)\phi'_i = \lambda'_i \phi'_i , \quad \lambda'_i = 1 + K/\rho_i , \quad (3.6)$$

$$\phi'_i(n) = (-1)^{n_1 + n_2 + n_3 + n_4} \phi_i(n) .$$

Here n_i are the coordinates of the site which corresponds to n .

(F4). For one zero mode, there are 15 associated zero modes. They are reminiscent of species doubling.

(F5). If ϕ_i is an eigenfunction with eigenvalue λ_i , then

$$\phi_i^\dagger \gamma_5 D = \lambda_i^* \phi_i^\dagger \gamma_5 . \quad (3.7)$$

(F6). Orthogonal relations are given by

$$(\phi_i^\dagger \gamma_5 \phi_j) = 0 \quad \text{for } \lambda_i^* \neq \lambda_j. \quad (3.8)$$

Here we have introduced an abbreviated symbol

$$(\phi_i^\dagger \gamma_5 \phi_j) = \sum_n \phi_i^\dagger(n) \gamma_5 \phi_j(n).$$

(F7). The spectral representation of D^{-1} is given by

$$D^{-1}(n, m) = \sum_i \frac{1}{\lambda_i} \frac{\phi_i(n) \bar{\phi}_i^\dagger(m) \gamma_5}{(\bar{\phi}_i^\dagger \gamma_5 \phi_i)}. \quad (3.9)$$

(F8). The spectral representation of $(\gamma_5 D)^{-1}$ is given by

$$(\gamma_5 D)^{-1}(n, m) = \sum_i \frac{1}{\mu_i} \chi_i(n) \chi_i^\dagger(m). \quad (3.10)$$

(F9). The following relations between the eigenvalues and eigenfunctions of D and $\gamma_5 D$ are satisfied: As $K \rightarrow \rho_i$ (complex in general),

$$\begin{aligned} \mu_i &= \lambda_i \frac{(\bar{\phi}_i^\dagger \gamma_5 \phi_i)}{(\bar{\phi}_i^\dagger \phi_i)} + O(\lambda_i^2), \\ \chi_i &= \phi_i + O(\lambda_i). \end{aligned} \quad (3.11)$$

IV. TOPOLOGICAL CHARGE AND ZERO MODES

The Atiyah-Singer theorem¹⁶ holds in the continuum theory

$$Q = n_+ - n_-. \quad (4.1)$$

Here Q is the topological charge defined by

$$Q = \frac{1}{32\pi^2} \int d^4x F_{\mu\nu}^a(x) \bar{F}_{\mu\nu}^a(x), \quad (4.2)$$

and n_+ (n_-) is the number of zero modes of the quark field with positive (negative) chirality for the eigenvalue equation

$$\gamma_\mu (\partial_\mu - ig A_\mu) \psi = \lambda \psi. \quad (4.3)$$

The chirality is defined by the eigenvalue of γ_5 :

$$\gamma_5 \psi = \pm \psi. \quad (4.4)$$

In this section we investigate how relation (4.1) is modified and how it is realized on a lattice.

In general, the concept of topology has no intrinsic meaning on a lattice. Only when the field configuration changes smoothly it has an intrinsic meaning. As mentioned earlier a few years ago we proposed¹⁴ a definition for SU(2) topological charge. (Note that at that time only the Lüscher's¹⁷ definition had been known.) At that time, similar but slightly different definitions for SU(2) topological charge were proposed by Polonyi¹⁸ and Woit,¹⁹ independently. We found that the definition by Woit is better than ours and Polonyi's because the latter definition depends on the choice of the boundaries, and checked that relation (2.5) is well satisfied for the nontrivial solutions we found with Woit's definition. Any of these definitions reduces to the continuum one (4.2) in the continuum limit

$a \rightarrow 0$ when a gauge configuration is smooth in the sense that we can choose a gauge where the vector field $A_\mu(n)$ defined by

$$U(n, \mu) = \exp[iag A_\mu(n)] \quad (4.5)$$

is a smooth function of n :

$$\lim_{a \rightarrow 0} A_\mu(n) \rightarrow A_\mu(x), \quad (4.6)$$

where $x = na$ and $A_\mu(x)$ is differentiable.

For the SU(3) group which we are working with we use the method proposed by Parisi and Rapuano:²⁰ we decompose an SU(3) group element into a product of an SU(2) group element and an S^5 element and then apply Woit's definition of topological charge to the SU(2) group. We choose nine ways of embedding an SU(2) subgroup into an SU(3) group which are described in Eq. (10) of Ref. 20. Seven or eight choices give identical values for smooth gauge configurations, while one or two give different ones. This is due to the fact that some decompositions are singular. We use the majority rule.

Let us consider the eigenvalue equation on a lattice:

$$D(K) \phi_i = \lambda_i \phi_i, \quad (4.7)$$

where $D(K)$ is given by Eq. (2.2). In the lattice theory with Wilson fermion action, the Wilson term violates chiral symmetry. Hence, zero modes of the eigenvalue equation (4.7) are not eigenfunctions of chirality but approximately eigenfunctions:

$$\gamma_5 \phi \approx \pm \phi. \quad (4.8)$$

Therefore we define the chirality χ of a zero mode by the sign of $(\phi^\dagger \gamma_5 \phi)$:

$$\chi = \text{sgn}(\phi^\dagger \gamma_5 \phi). \quad (4.9)$$

In the continuum limit [$a \rightarrow 0$ and $K \rightarrow K_c (\beta = \infty) = \frac{1}{8}$] the eigenvalue equation (4.7) reduces to the continuum one (4.3) except for the normalization factor $\frac{1}{4}$ ($= 2K_c$), if the gauge configuration is smooth in the sense defined above. In this case, zero modes are eigenstates of chirality defined by Eq. (4.4) and therefore the chirality defined by the sign of $(\phi^\dagger \gamma_5 \phi)$ also reduces to the continuum one.

To obtain the number of zero modes for a given configuration, we have investigated eigenvalues of Hermitian matrix $\gamma_5 D$ by Lanczos method. If a real eigenvalue of D is zero at K_c , the corresponding eigenvalue of $\gamma_5 D$ is also zero at K_c . The eigenvalue of Hermite operator $\gamma_5 D$ is real and changes its sign when K crosses K_c . It may be worthwhile to emphasize that the sign change implies the existence of the exact zero eigenvalue. On the other hand, the eigenvalues of $\gamma_5 D$ which correspond to complex eigenvalues of D cannot become zero for any real K . See Fig. 1 for some typical examples. Furthermore we can determine the chirality of a zero mode from the slope of the eigenvalue of $\gamma_5 D$ at K_c , because the eigenvalue λ of D and the eigenvalue μ of $\gamma_5 D$ are related with the factor $(\phi^\dagger \gamma_5 \phi)$ at $K = K_c$ [see (F9) in Sec. III]:

$$\mu = \lambda (\phi^\dagger \gamma_5 \phi) + O(\lambda^2). \quad (4.10)$$

For the Wilson quark at finite β , it is not obvious which

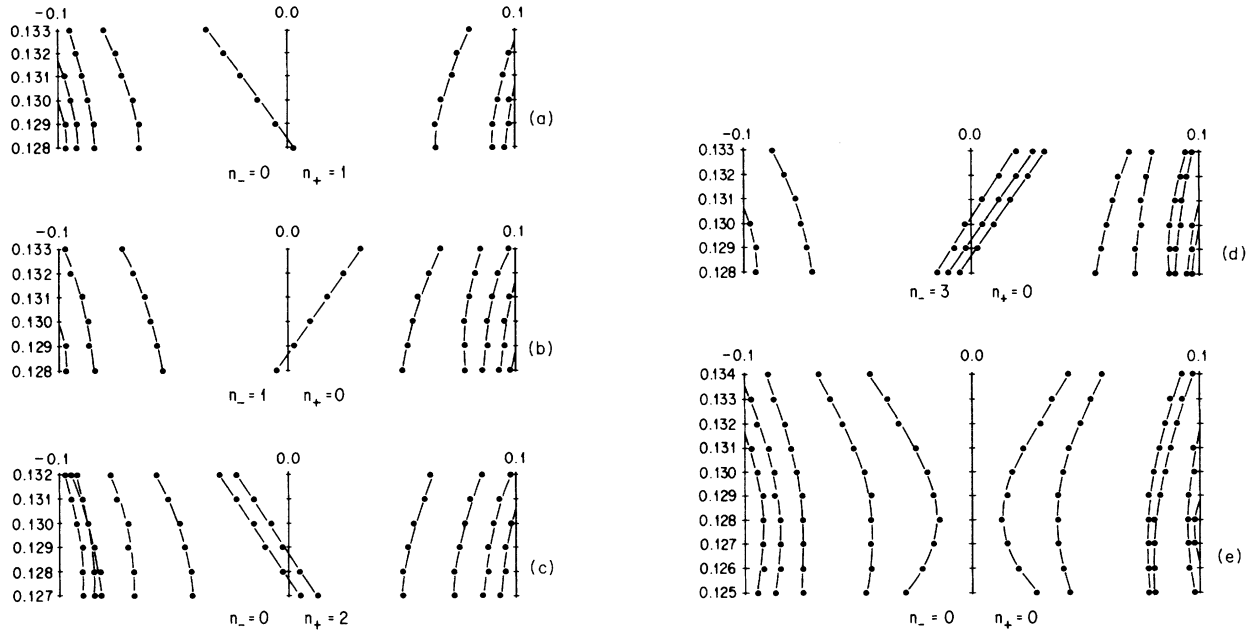


FIG. 1. Eigenvalues μ of $\gamma_5 D$ ($-0.1 \leq \mu \leq 0.1$) vs K for various configurations at $\beta \approx \infty$ on an $8^3 \times 16$ lattice.

K corresponds to the massless quark. Related with this, although the K_c^{ensemble} where the pion mass vanishes on the ensemble average is unique, K_c for each configuration scatters around K_c^{ensemble} . For example, at $\beta=2.4$ on an $8^3 \times 16$ lattice, $0.157 \lesssim K_c \lesssim 0.159$. [Note that K_c^{ensemble} is about 0.1569(2) which has been obtained from the hadron spectrum calculation on a $16^3 \times 48$ lattice.²¹ We expect that the K_c for each configuration is larger than this value. All the K_c 's roughly satisfy this condition. However, some of them are slightly less than this. We interpret this as a finite-size effect.] If there are more than two K_c 's around K_c^{ensemble} for a configuration, they do not in general coincide. As mentioned above, in the continuum limit ($a \rightarrow 0$) K_c for a smooth gauge configuration should approach $\frac{1}{8}$.

Let us discuss the problem related with species doubling. If there is one zero mode with chirality χ around K_c^{ensemble} ($1/K > 4$), there exist 15 associated zero modes in the “unphysical region” ($1/K < 4$): four (with $-\chi$) for $2 \leq 1/K < 4$, six (with $+\chi$) for $-2 \leq 1/K \leq 2$, four (with $-\chi$) for $-4 < 1/K \leq -2$, and one (with $+\chi$) for $1/K < -4$. This is reminiscent of species doubling. We have checked numerically the existence of these zero modes for several configurations. We list in Table I, as an example, 15 zero modes associated with one K_c for a gauge configuration on a 6^4 lattice at $\beta=2.4$.

From the above analysis we may expect that an analogue of the Atiyah-Singer index theorem

$$“n_+” - “n_-” = “Q” \quad (4.11)$$

holds when β is large by the following reason. Here “ n_+ ” (“ n_- ”) is the number of zero modes around K_c^{ensemble} ($1/K > 4$) with positive (negative) “chirality” defined by the sign of $(\phi^\dagger \gamma_5 \phi)$, and “ Q ” is the topological

charge on a lattice. As mentioned earlier, the topological charge “ Q ” and the eigenvalue equation on a lattice reduce to the continuum ones in the continuum limit if a gauge configuration is smooth. If β is large, smooth gauge configurations will dominate the gauge ensemble, and therefore for almost all configurations the index theorem on a lattice will be satisfied.

We have first examined the relation between the topological charge and the number of the zero modes on an $8^3 \times 16$ lattice for 16 gauge configurations which have been generated at $\beta=2.4$ and have been cooled down to $\beta \approx \infty$ by 100 iterations as explained in Ref. 14. Because these configurations are smooth, topological charges are

TABLE I. 15 zero modes associated with one K_c for a gauge configuration on a 6^4 lattice at $\beta=2.4$.

Region	K_c	Chirality
$1/K > 4$	0.156 828	+
	0.301 447	
$4 > 1/K > 2$	0.308 929	-
	0.313 510	
	0.319 829	
$2 > 1/K > 0$	8.073 44	+
	14.990 82	
$0 > 1/K > -2$	74.554 2	+
	-74.554 2	
$-2 > 1/K > -4$	-14.990 82	-
	-8.073 44	
	-0.319 829	
$-4 > 1/K$	-0.313 510	+
	-0.308 929	
	-0.301 447	
	-0.156 828	

definitely calculated. We have also measured the chirality of the zero modes in the physical hopping-parameter region ($1/K > 4$) for the same gauge configurations. We present these results in Table II. We find that the topological charge agrees with the number of the zero modes with positive chirality minus that with negative chirality for each configuration. Thus we confirm that the Atiyah-Singer theorem holds on a lattice at least at $\beta \approx \infty$. (Note that we have found a gauge configuration with $n_+ = 1$ and $N_- = 1$ after cooling by 100 iterations. However, when the configuration has been cooled down completely it has reduced to the trivial configuration. Thus we find no exact solutions such that instantons and anti-instantons coexist on a lattice.)

The relation between the topological charge and the number of the zero modes becomes more subtle at finite β than at $\beta \approx \infty$. The configurations at $\beta = 2.4$ are not smooth enough for unambiguous determination of the topological charge by the Parisi-Rapuno-Woit definition. Therefore we have measured the topological charge of gauge configurations after cooling the configurations. In this case, about one-half of 50 configurations satisfy the relation (4.11) with this "topological charge" (see below for more details). Because it is not guaranteed that the cooling process preserves the topological property of a gauge configuration, this disagreement does not imply that the relation (4.11) is not satisfied for finite β . If we were able to use other definitions which can determine definitely the topological charge for any configuration without cooling, the index theorem would be satisfied for more gauge configurations at $\beta = 2.4$.

Here we rather propose to define the topological charge of a gauge configuration on a lattice by the number of the zero modes with positive chirality minus that with negative chirality in the physical hopping-parameter region:

$$Q \equiv "n_+" - "n_-". \quad (4.12)$$

We use this definition in the following. Note that in Ref. 22 the Atiyah-Singer theorem for Wilson fermions is investigated from a different viewpoint.

TABLE II. Topological charge and the number of the zero modes for 16 gauge configurations on an $8^3 \times 16$ lattice at $\beta \approx \infty$.

No.	"Q"	"n ₊ "	"n ₋ "
1	-2	0	2
2	1	1	0
3	3	3	0
4	2	2	0
5	3	3	0
6	2	2	0
7	1	1	0
8	1	1	0
9	-1	0	1
10	-3	0	3
11	-1	0	1
12	0	1	1
13	0	0	0
14	0	0	0
15	0	0	0
16	0	0	0

We have also investigated the eigenfunctions of D . By making use of power method of D^{-1} , we obtain the eigenfunction for the smallest eigenvalue of D . If a real eigenvalue of D is smaller than the absolute magnitudes of complex eigenvalues at K which we choose to apply power method, as shown in Fig. 2(a), it is not difficult to obtain a real eigenvalue and the corresponding eigenfunc-

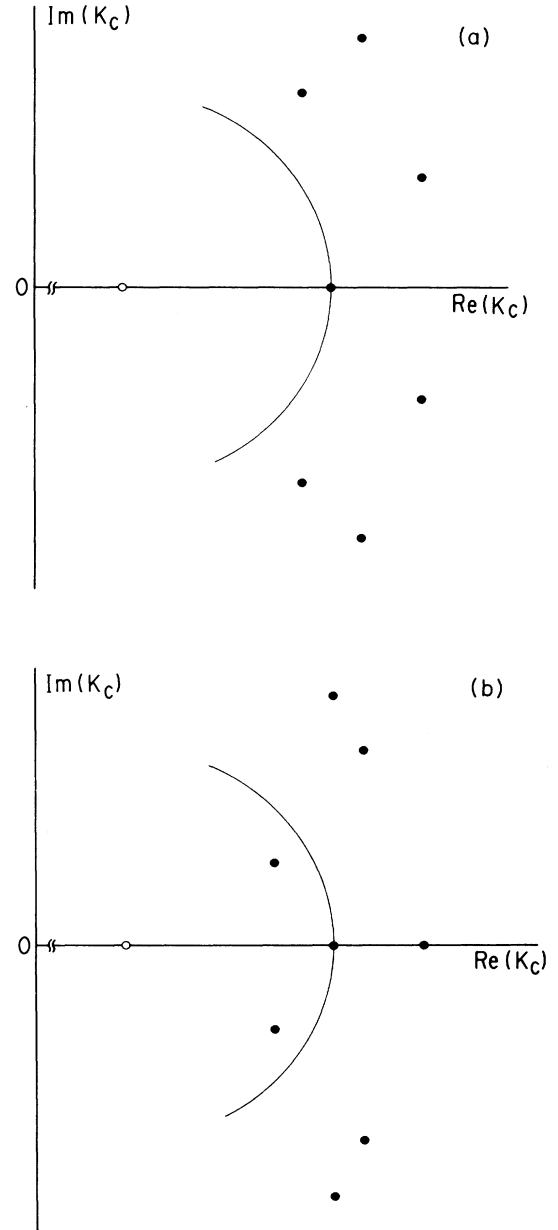


FIG. 2. Schematic graph for the eigenvalues of D . Solid circles indicate poles of D^{-1} in K . The open circle indicates the hopping parameter which is chosen in D for the power method. The distance between the open circle and a solid circle represent the absolute magnitude of the corresponding eigenvalue: The real eigenvalue is the smallest eigenvalue in absolute magnitude for (a), while a pair of complex eigenvalues are for (b).

tion by a power method. If not, as shown in Fig. 2(b), it is difficult. [We have checked that the case in Fig. 2(b) really happens.] We have tried to obtain the eigenfunctions up to the second smallest eigenvalues, using Schmidt's orthogonalization, for 50 configurations at $\beta=2.4$. The third smallest ones have not been searched for. With these limitations, we have just compared the number of zero modes with the "topological charge" measured as explained above. Then we find that about one-half of 50 configurations satisfy the index theorem, as mentioned earlier. Therefore we may say that more than one-half of them satisfy the index theorem with this "topological charge." Of course, K_c 's and the chiralities of the zero modes obtained by power method agree with those obtained by the Lanczos method.

We have searched for topologically trivial configurations ($n_+ = n_- = 0$). We have found only one trivial configuration. Thus topologically nontrivial configurations dominate 50 configurations. This is natural because the entropy of topologically nontrivial configurations [for example, that due to the position in space and the orientation in SU(3) gauge group of topological excitations] is large.

In order to see how the zero modes are approximately eigenstates of chirality, we have calculated the value

$$\chi_l = \frac{\phi^\dagger \gamma_5 \phi}{\phi^\dagger \phi}. \quad (4.13)$$

$|\chi_l| \approx 0.92-0.97$ at $\beta \approx \infty$ and $|\chi_l| \approx 0.5-0.7$ at $\beta=2.4$. We see that as β becomes large, the zero modes approach exact eigenstates of chirality as expected.

V. SCALAR DENSITY AND PSEUDOSCALAR DENSITY

The contributions from each configuration to the expectation values of the scalar density and the pseudoscalar density are given by

$$\bar{\psi}(n)\psi(n) = \text{Tr}[D^{-1}(n,n)] \quad (5.1)$$

and

$$\bar{\psi}(n)\gamma_5\psi(n) = \text{Tr}[D^{-1}(n,n)\gamma_5], \quad (5.2)$$

respectively. Here, the summation over n is not taken.

Let us consider the quark propagator on a topologically nontrivial gauge configuration. Let us assume that a real eigenvalue becomes zero at $K = K_c$. Then, as $K \rightarrow K_c$,

$$D^{-1}(n,m) \sim \frac{1}{1-K/K_c} \frac{\phi(n)\phi^\dagger(m)\gamma_5}{\phi^\dagger\gamma_5\phi}, \quad (5.3)$$

where ϕ is the corresponding eigenfunction. From Eqs. (5.1)–(5.3) we have

$$\bar{\psi}(n)\psi(n) \sim \frac{1}{1-K/K_c} \frac{\phi^\dagger(n)\gamma_5\phi(n)}{\phi^\dagger\gamma_5\phi}, \quad (5.4)$$

$$\bar{\psi}(n)\gamma_5\psi(n) \sim \frac{1}{1-K/K_c} \frac{\phi^\dagger(n)\phi(n)}{\phi^\dagger\gamma_5\phi}. \quad (5.5)$$

As mentioned in Sec. IV, any zero mode is also approximately an eigenfunction of γ_5 : $\phi^\dagger(n)\gamma_5\phi(n) \approx \pm\phi^\dagger(n)\phi(n)$. Thus as K approaches K_c , both the scalar density and the

pseudoscalar density become large and diverge at $K = K_c$. [Note that the magnitude of the pseudoscalar density $\bar{\psi}(n)\gamma_5\psi(n)$ becomes eventually larger than the scalar density $\bar{\psi}(n)\psi(n)$, because $\phi^\dagger(n)\phi(n) \geq |\phi^\dagger(n)\gamma_5\phi(n)|$.] The contribution of other terms in the spectral representation are approximately constants around K_c . Therefore, we predict the K dependence of the scalar density and the pseudoscalar density around $K = K_c$ as

$$\bar{\psi}(n)\psi(n) = \frac{a_s}{1-K/K_c} + b_s, \quad (5.6)$$

$$\bar{\psi}(n)\gamma_5\psi(n) = \frac{a_p}{1-K/K_c} + b_p. \quad (5.7)$$

We have checked numerically this prediction for various configurations. We present the results of a typical configuration ($Q=1$ on a 6^4 lattice) in Fig. 3. The scalar and pseudoscalar densities at $n=0$ which are obtained from the quark propagator by Eqs. (5.1) and (5.2) are plotted versus the inverse eigenvalue $(1-K/K_c)^{-1}$. They are remarkably linear and we obtain

$$\bar{\psi}(0)\psi(0) = 0.000302(1-K/K_c)^{-1} + 10.9, \quad (5.8)$$

$$\bar{\psi}(0)\gamma_5\psi(0) = 0.000423(1-K/K_c)^{-1} - 0.0339, \quad (5.9)$$

by the fit to the form of Eqs. (5.6) and (5.7), respectively. On the other hand, from the eigenfunction we have

$$\phi(0)\phi(0) = 0.0002799, \quad (5.10)$$

$$\phi(0)\gamma_5\phi(0) = 0.0001999, \quad (5.11)$$

$$(\phi^\dagger\gamma_5\phi) = 0.66128, \quad (5.12)$$

with the normalization $(\phi^\dagger\phi) = 1.0$. Thus, the factors for $(1-K/K_c)^{-1}$ determined numerically from Fig. 3 in the both cases of the scalar and pseudoscalar densities, as given in Eqs. (5.8) and (5.9), are in remarkable agreement with those calculated from Eqs. (5.10)–(5.12) with the use of Eqs. (5.4) and (5.5).

We also show the scalar density and the pseudoscalar density at $n=0$ versus the hopping parameter for a wide range in Fig. 4 (see also Fig. 5 with a different horizontal

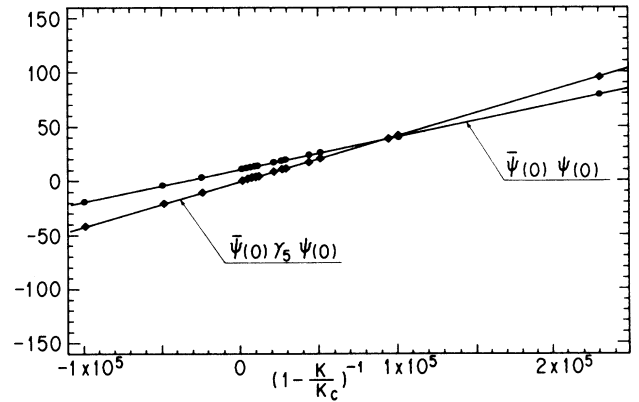


FIG. 3. The scalar density $\bar{\psi}(0)\psi(0)$ and the pseudoscalar density $\bar{\psi}(0)\gamma_5\psi(0)$ vs $(1-K/K_c)^{-1}$ for a gauge configuration with $Q=1$ on a 6^4 lattice at $\beta=2.4$.

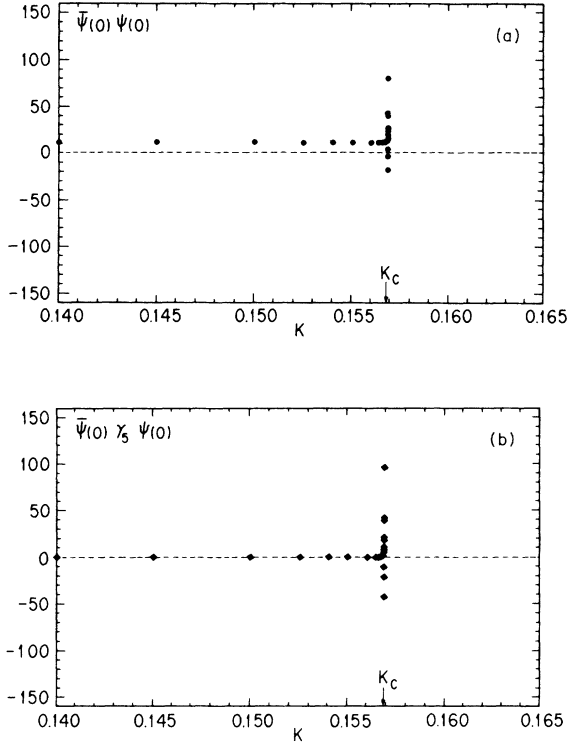


FIG. 4. The same as Fig. 3 except for the horizontal scale being replaced with K : (a) The scalar density; (b) the pseudoscalar density.

scale from that of Fig. 4). The hopping-parameter region where we have extensively calculated the hadron spectrum is^{11,21,23} $0.14 \leq K \leq 0.154$. In this region, the pseudoscalar density is much smaller than the scalar density which is of order 10. In the very narrow region around K_c , the pseudoscalar density rapidly becomes large together with the scalar density. Note that the densities change their signs due to the factor $(1 - K/K_c)^{-1}$ when K crosses K_c . We have obtained similar results for many topologically nontrivial configurations on various lattices (4^4 , 6^4 , 8^4 , and $8^3 \times 16$).

For a topologically trivial gauge configuration we cannot expect that the pseudoscalar density becomes comparable to the scalar density because there are no poles in D^{-1} for real K . We represent the result for a topologically trivial configuration on a 6^4 lattice in Fig. 6. The spikes observed for the case of the topologically nontrivial configuration do not appear in this case. For the whole region of K , even above K_c^{ensemble} (~ 0.1569), where the quark propagators are calculated, the pseudoscalar density is of order 10^{-2} and the scalar density is of order 10. For a topologically trivial configuration there is no term which dominates in the spectral representation of the propagator. In fact, we have found four pairs of complex eigenvalues around $\text{Re}(K_c) \simeq 0.157 - 0.158$, which are shown in Fig. 7. Even if we take into account these eight terms the spectral representation of the propagator does not approximate the behavior of D^{-1} around K_c^{ensemble} . This is quite different

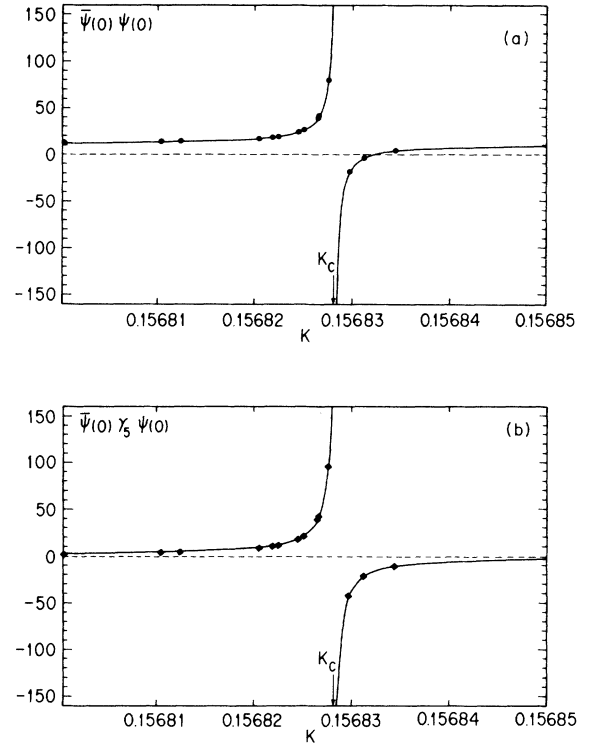


FIG. 5. The same as Fig. 4. The hopping-parameter region is narrower than that in Fig. 4. The solid curves represent the fits given in Eqs. (5.8) and (5.9).

from the situation for the $Q=1$ configuration where one pole dominates the propagator at $K \sim K_c$.

From the above we conclude as follows: Only for the topologically nontrivial gauge configurations and only when K is very close to K_c^{ensemble} , the pseudoscalar density becomes comparable to the scalar density.

VI. HADRON PROPAGATORS

The propagators of the η meson and the π meson are given by

$$G_\eta(0, n) = G^C(0, n) - N_f G^{DC}(0, n) \quad (6.1)$$

and

$$G_\pi(0, n) = G^C(0, n), \quad (6.2)$$

where

$$G^C(0, n) = \langle \text{Tr}[D^{-1}(0, n)\gamma_5 D^{-1}(n, 0)\gamma_5] \rangle \quad (6.3)$$

and

$$G^{DC}(0, n) = \langle \text{Tr}[D^{-1}(0, 0)\gamma_5] \text{Tr}[D^{-1}(n, n)\gamma_5] \rangle. \quad (6.4)$$

Here N_f is the number of flavors with degenerate small quark mass. In our case $N_f=2$. The fact that $m_\eta \gg m_\pi$ means that there is a large cancellation between G^C and G^{DC} , because the π propagator is a slowly decaying function of n , while the η propagator is a rapidly decaying

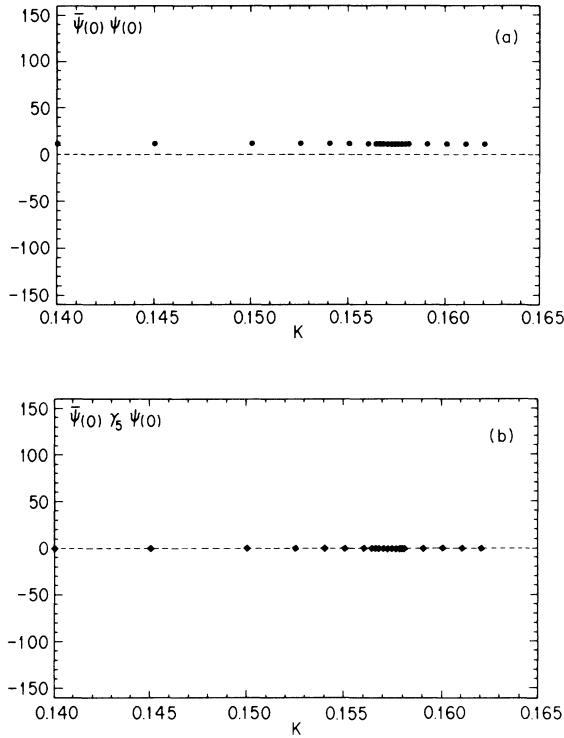


FIG. 6. The scalar density (a) and the pseudoscalar density (b) vs K for a topologically trivial gauge configuration on a 6^4 lattice at $\beta=2.4$.

function. However, the disconnected part $G^{DC}(0,0)$ is much smaller than the connected part $G^C(0,0)$ by a factor of 10^{-5} – 10^{-6} in the hopping region where the hadron spectrum was calculated.

The disconnected part G^{DC} is the correlation function of the pseudoscalar density. Therefore when the pseudoscalar density is large, G^{DC} will become large. Hence, the contribution to G^{DC} from a topologically nontrivial configuration will become large as $K \rightarrow K_c$ and will diverge at $K = K_c$. The leading terms of G^C and G^{DC} for such a configuration are double-pole terms and identical. Thus G^{DC} becomes comparable to G^C , as $K \rightarrow K_c$. Because topologically nontrivial configurations dominate the ensemble, this will be the resolution of the U(1) problem.

It should be noted that the argument given above does not depend on how a gauge configuration is generated: in the quenched approximation or in the unquenched calculation. (See below for more discussion.) Thus, in order to confirm the above conjecture we have investigated the η propagators as well as the π propagators on an $8^3 \times 16$ lattice at $\beta=2.4$ for ten gauge configurations which are generated by a Cabibbo-Marinari algorithm slightly modified for vector processors²⁴ in the quenched approximation, separated by 500 sweeps after thermalization. Only one of them is topologically trivial ($n_+ = n_- = 0$) and the others are topologically nontrivial. We have calculated $G^C(0,0;0,t)$ and $G^{DC}(0,0;0,t)$ without taking Fourier transformation, because it would be very time consuming to make Fourier transformation and it is possible to determine the ground-state mass from the long-distance behav-

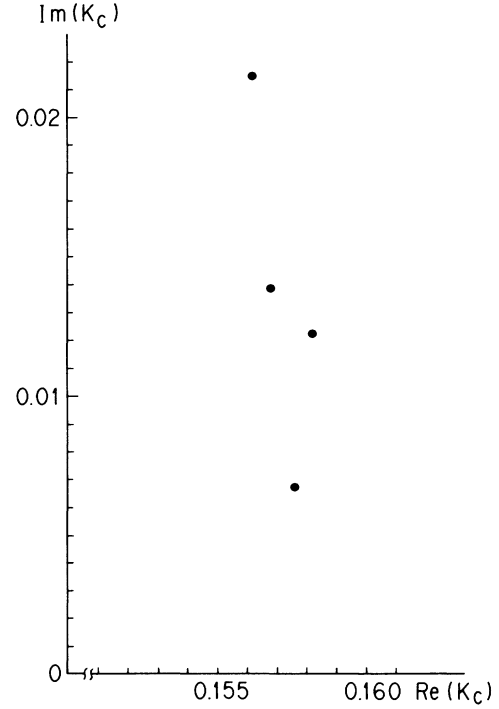


FIG. 7. Poles of D^{-1} around $\text{Re}(K_c) \approx 0.157$ – 0.158 for the same configuration as in Fig. 6. We represent only the complex poles for which the real part is positive.

ior of the propagator $e^{-mt}/t^{3/2}$. We have calculated 16 quark propagators, taking the origin at different points in the temporal direction with spatial coordinates fixed. We have used a slightly modified version of the conjugate residual method with an incomplete (LU) (lower and upper triangular matrices) decomposition which is described in Appendix B to solve the quark propagator. Then we take the average of 16 $G^C(0,n)$ and $G^{DC}(0,n)$ which are obtained from the quark propagators. In this way we obtain the $G^C(0,n)$ and the $G^{DC}(0,n)$ with spatial coordinates fixed for a gauge configuration, as the averages of 16 $G^C(0,n)$ and $G^{DC}(0,n)$. Finally we take the ensemble average of the results thus obtained for 10 configurations. To estimate the statistical errors we treat the average for each configuration as statistically independent. We have calculated the propagators for all of 10 configurations at $K=0.14, 0.145, 0.15, 0.1525, 0.154, 0.156, \text{ and } 0.1564$.

We show in Fig. 8 the G^C and G^{DC} at some selected hopping parameters (because seven of them would be too much) which are obtained as the ensemble average for 10 configurations. From the figure we are really able to confirm that the $G^{DC}(0,n)$ becomes comparable to the $G^C(0,n)$ at $4 \leq t \leq 12$ when K approaches K_c^{ensemble} .

Let us next calculate the η propagator. The problem we have to be concerned with is the validity of the quenched approximation for the calculation of the flavor-singlet meson mass. Generally speaking, the effect of quark loops is crucial for the η - π splitting. Therefore the issue is how much we can absorb the effect of quark loops by renormalizing β . We here assume as a working hy-

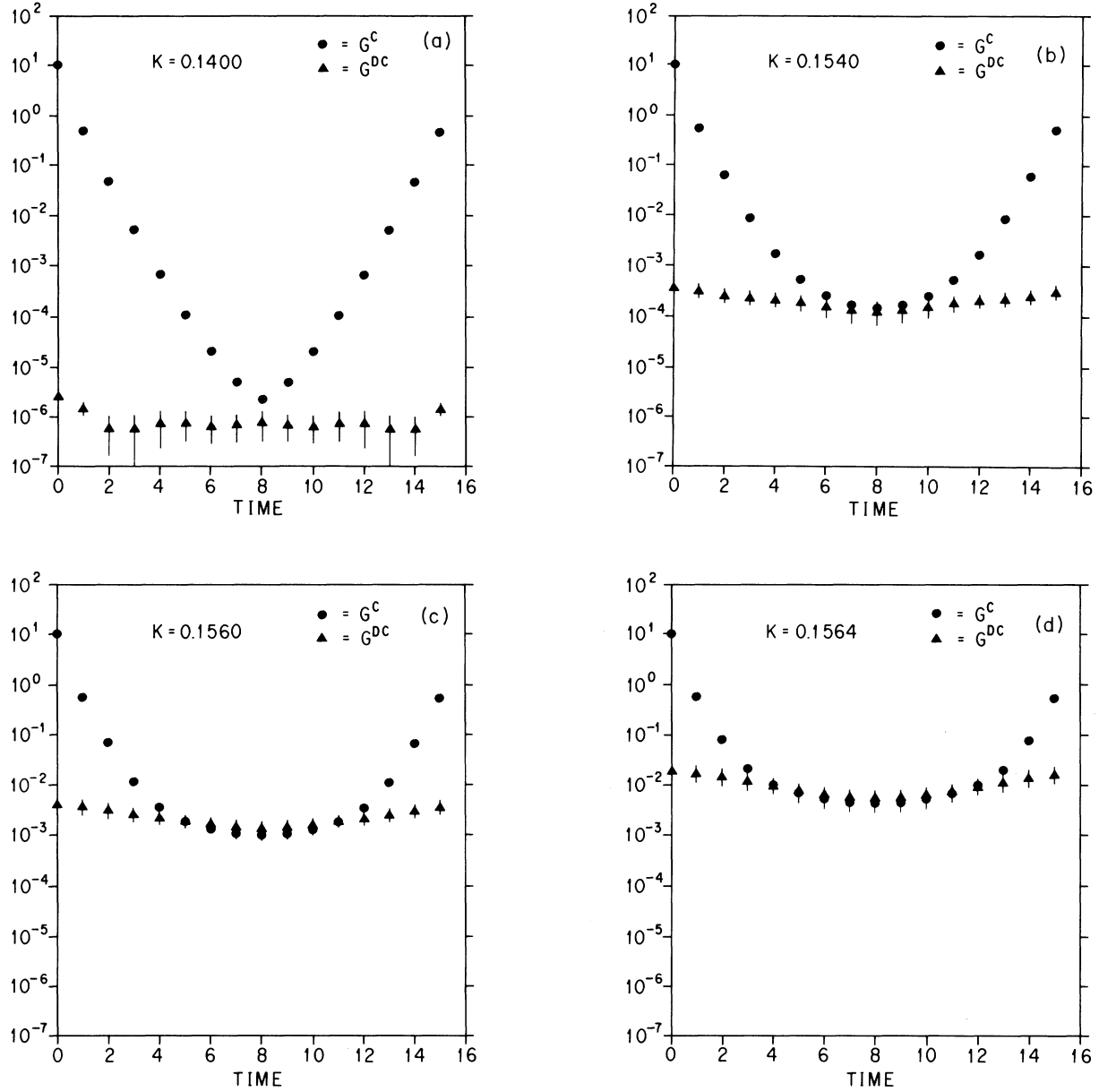


FIG. 8. The $G^C(\mathbf{0}, t; 0)$ and $G^{DC}(\mathbf{0}, t; 0)$ for the ensemble average at several selected hopping parameters.

pothesis that the behavior $G^C \sim C_1 e^{-m_\pi t}$ and $G^{DC} \sim C_2 e^{-m_\pi t} + C_3 e^{-m_\eta t}$ is valid even in the quenched approximation by renormalizing β , although the constants C_1 , C_2 , and C_3 are different from those in the unquenched calculation. This assumption can be checked *a posteriori*. (Further discussion about this assumption will also be given elsewhere.²⁵) Then the η propagator is given by Eq. (6.1) only by replacing the constant N_f with $\zeta = C_1/C_2$. The constants C_1 , C_2 , and C_3 and therefore the constant ζ should be determined for the ensemble average. We see from Fig. 8 that the assumption on the behavior of the G^C and the G^{DC} is well satisfied for these propagators when K is close to K_c^{ensemble} ; the G^{DC} for $5 \leq t \leq 11$ is similar to the G^C except for the normalization

constant. Therefore we determine the ζ by simply equating $\zeta = G^C(t=8)/G^{DC}(t=8)$, because at $t=8$ the η propagator should be very small. (For small hopping parameters such that $\zeta > 2.0$ we set $\zeta = 2.0$.)

In Fig. 9 we display the η propagators determined in this way together with the π propagators at the selected hopping parameters. (Note that the G_η at $t=8$ is missing because of the method of the determination of ζ . Of course, we can make a fine-tuning of ζ in such a way that the G_η looks smooth even at $t=8$. For example, at $K=0.1564$, if we change from $\zeta=0.73553$ to $\zeta=0.73383$, we obtain the G_η shown in Fig. 10.) We also show in Fig. 11 the ρ and ω propagators at $K=0.1564$ which have been obtained by a similar method

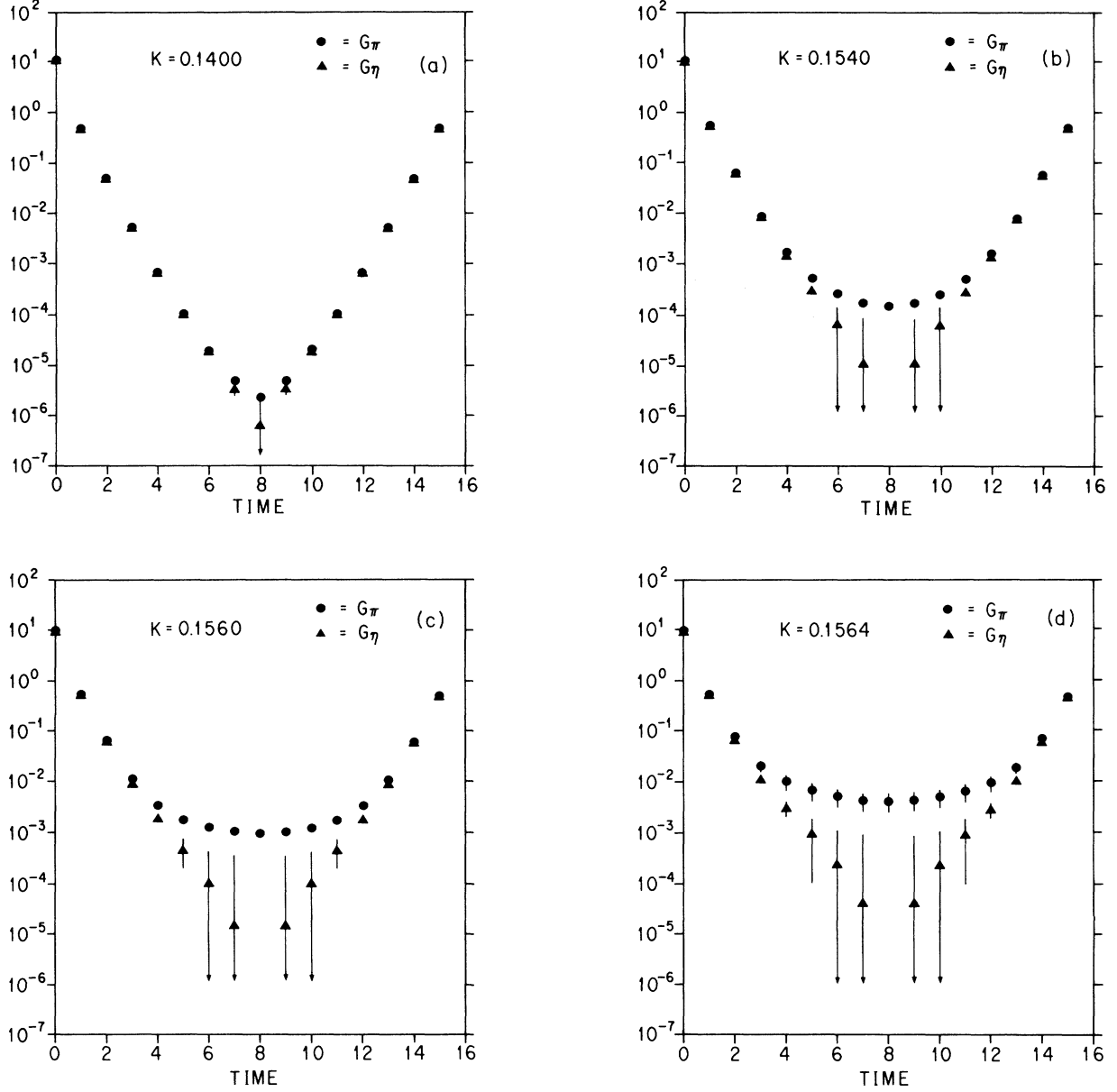


FIG. 9. The η and π propagators without Fourier transformation for the ensemble average at the same hopping parameters as in Fig. 8.

with the same ζ . We would like to emphasize that the η propagators thus obtained are well behaved: If our working hypothesis is not valid, they will not look like propagators. Thus this *a posteriori* justifies our assumption. We notice the following. (i) The η propagator clearly starts to deviate from the π propagator as $K \rightarrow K_c^{\text{ensemble}}$ and is approximately identical to the ρ propagator at $K=0.1564$ which is nearly equal to K_{phy} according to the calculation of the hadron spectrum on a $16^3 \times 48$ lattice²¹ (K_{phy} is the hopping-parameter value where m_ρ/m_π takes the physical value). It is interesting to note that the η propagators do not change noticeably even if we change the hopping parameter from 0.154 to 0.1564. This means that the mass of the η is almost constant from $K=0.154$

to 0.1564, while the mass of the π decreases very fast. (ii) There are no noticeable differences between the ρ and ω propagators up to $K=0.1564$. At $K=0.1564$ ($\simeq K_{\text{phy}}$), m_ρ (m_ω) is several times larger than m_π : This can be seen from Figs. 9 and 11. Thus we conclude that m_η is comparable to m_ρ and is several times m_π .

Next, let us discuss how large the contribution from each configuration to the G^{DC} is. To do so we show in Fig. 12 the contributions to the G^{DC} from a topologically nontrivial configuration ($Q=1$) and from the topologically trivial one at $K=0.1564$. We see the contribution from the topologically trivial one is much smaller than that from the $Q=1$ configuration. The contributions from the other topologically nontrivial ones are similar to that from

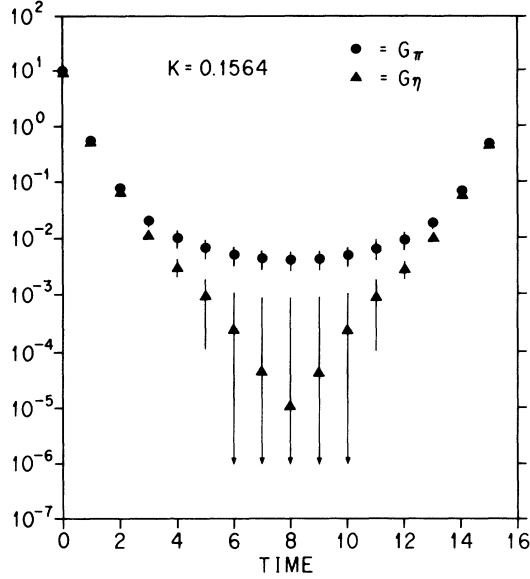


FIG. 10. The η and π propagators without Fourier transformation at $K=0.1564$ after a fine-tuning of ζ .

the $Q=1$ configuration.

Thus we conclude that the large splitting between the η mass and the π mass is caused both by the existence of topologically nontrivial configurations and by the fact that K_{phy} is very close to K_c^{ensemble} .

Let us make two comments. (i) In addition to the seven hopping parameters mentioned above, we have calculated the propagators for each configuration at several other hopping parameters which are very close to the K_c of each configuration. (Of course, we have not calculated the propagators for the other configurations at the hop-

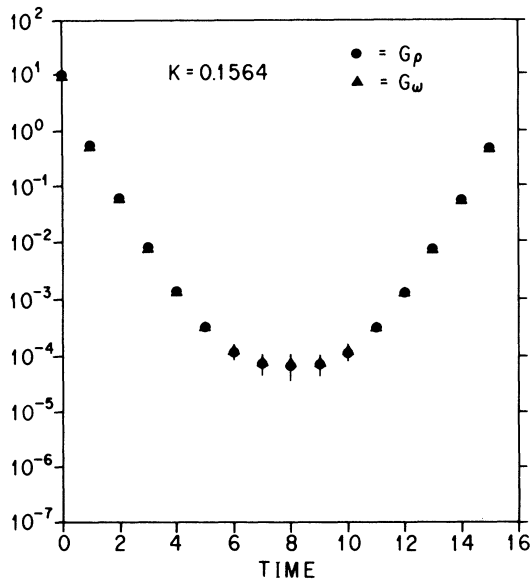


FIG. 11. The ρ and ω propagators without Fourier transformation at $K=0.1564$.

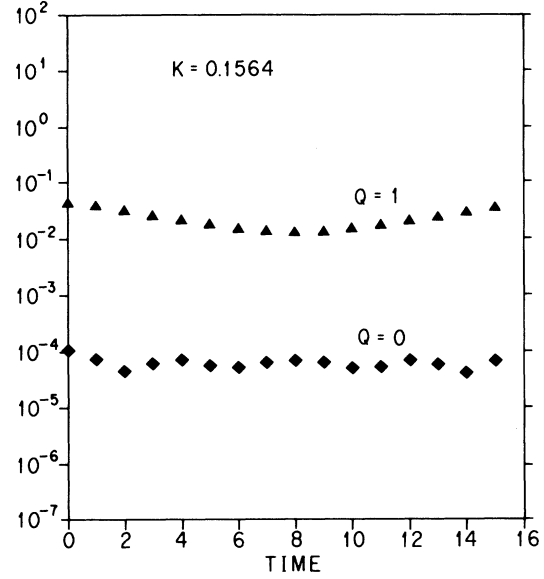


FIG. 12. The contribution to the G^{DC} from a topologically nontrivial configuration ($Q=1$) and a topologically trivial configuration ($Q=0$).

ping parameter which is very close to the K_c , because the K_c for each configuration differs from each other as mentioned earlier.) For a $Q=1$ configuration ($K_c=0.156757$), we have calculated G^C and G^{DC} at 14 K 's up to the point where the smallest eigenvalue becomes 10^{-5} . When the smallest eigenvalue is greater than 10^{-2} , the G^{DC} is negligible compared with the G^C . As K approaches toward K_c , the G^{DC} becomes larger and comparable to the G^C , and when $K \sim K_c$, the G^{DC} is almost identical with the G^C , as conjectured. See Fig. 13 and Table III. The results for other topologically nontrivial configurations are essentially identical. (ii) Because the K_c for each configuration slightly differs from each other, the G^{DC} fluctuates considerably. Nevertheless, the G^C and G^{DC} for the ensemble average look similar to those for each configuration.

TABLE III The eigenvalues of D vs the hopping parameters for a topologically nontrivial configuration ($Q=1$) with $K_c=0.156757$ (more precisely $K_c=0.15675675$).

K	λ
0.14	0.106 897
0.145	0.075 000
0.15	0.043 103
0.152 5	0.027 155
0.154	0.017 586
0.156	0.004 828
0.156 4	0.002 276
0.156 6	0.001 000
0.156 7	0.000 362
0.156 72	0.000 234
0.156 74	0.000 107
0.156 745	0.000 075
0.156 754	0.000 020
0.156 755	0.000 010

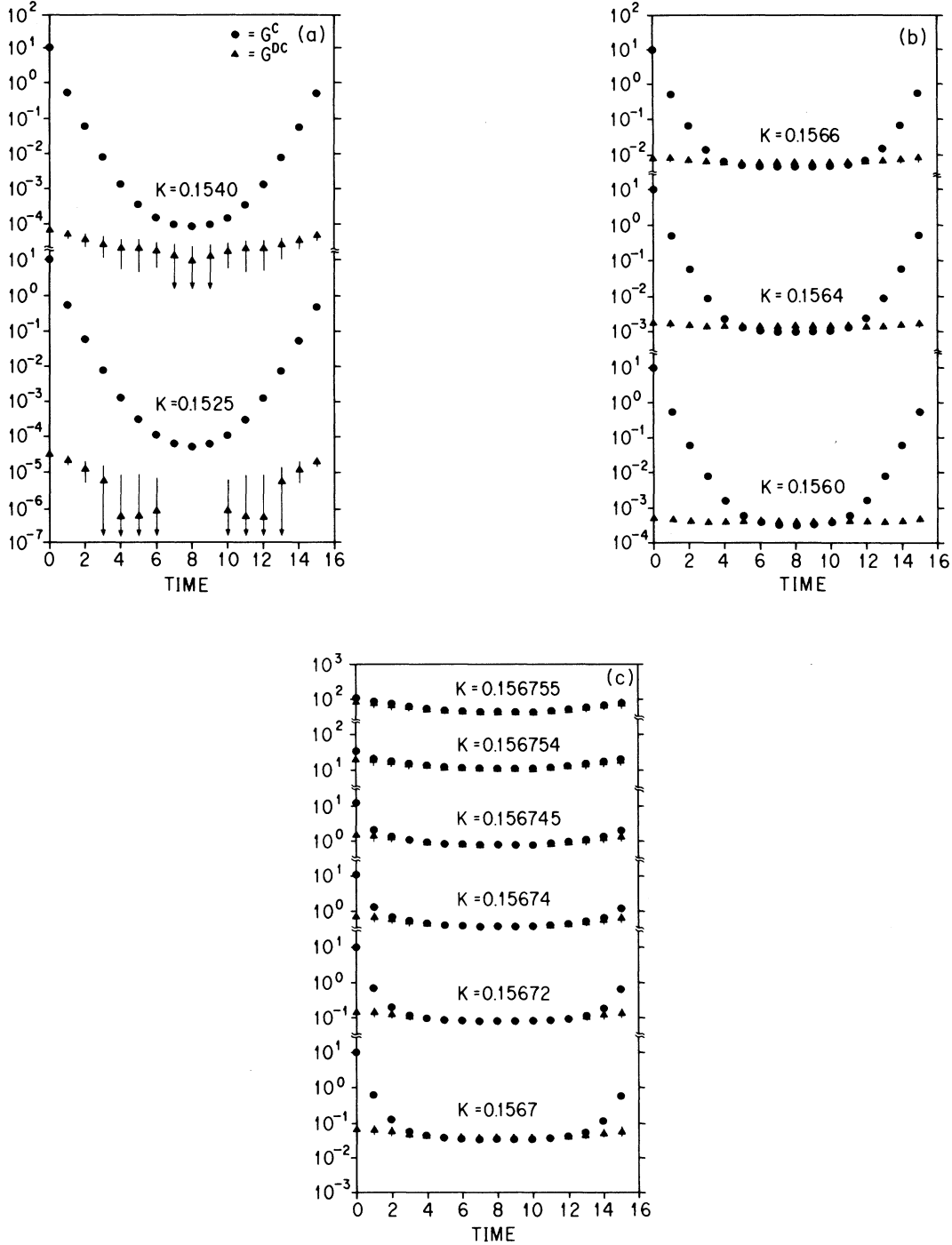


FIG. 13. The $G^C(0,t;0)$ and $G^{DC}(0,t;0)$ for a gauge configuration with $Q=1$ at various hopping parameters up to the one where the smallest eigenvalue of D becomes 10^{-5} . The errors in this figure are estimated by treating 16 data at different temporal coordinates as statistically independent. See the eigenvalues in Table III.

VII. THE MASSES OF THE η AND η' MESONS

In order to obtain the realistic value of the η' mass, we have to consider the mixing between our “ η ” $= (\bar{u}\gamma_5 u + \bar{d}\gamma_5 d)/\sqrt{2}$ and $\eta_s = \bar{s}\gamma_5 s$. We are able to obtain a very precise value for the mass of η_s including only the G^C

term, from the hadron-spectrum calculation on a $16^3 \times 48$ lattice.²¹ The hopping-parameter value which corresponds to the strange-quark mass is $K_s = 0.154$ which has been determined from the ϕ meson mass. The η_s mass turned out to be 700 MeV. Even if we include the effect of the G^{DC} term, the value only becomes slightly larger.

We estimate that the “ η ” mass and the η_s mass are roughly identical and about 750 MeV, because the propagators of the “ η ” ($K=0.1564$) and η_s ($K=0.154$) mesons are almost identical with those of the ρ and ω mesons at $K \simeq K_{\text{phy}}$, as mentioned in Sec. VI. (The lattice size $8^3 \times 16$ is not large enough to reduce completely finite-size effects and to determine the mass from the asymptotic behavior of the propagator. However, assuming the effects of finite-size effects are common to all of them and inputting the physical ρ mass 770 MeV, we obtain the estimated values for the “ η ” and η_s masses.) These values for the masses are in accord with the real world, because if we assume the transition mass matrix between the two states is about 200 MeV, we obtain the correct masses for the η' and η mesons and the mixing angle $\phi=10^\circ$ ($\eta'=\eta_1\cos\phi+\eta_8\sin\phi$) which is consistent with that obtained by phenomenological analyses. (See, for example, Ref. 26.) Note that we use neither the quadratic nor the linear Gell-Mann–Okubo mass formulas and neither of them agree with our results [$m(\eta') \simeq m(\eta_s) \simeq 750$ MeV].

Of course, in order to determine precisely the η' mass, we have to calculate the G^C and G^{DC} including the effects of dynamical quark loops on a larger lattice with high statistics. This is the problem to be investigated in the future.

VIII. DISCUSSION

A. The difference between 0^- and 1^- mesons

A natural question that arises is why is there a large splitting between m_π and m_η , while there is no noticeable splitting between m_ρ and m_ω . Let us first note that the contribution of a zero mode to $G^{DC}(0,n)$ is proportional to

$$\phi^\dagger(0)\phi(0)\phi^\dagger(n)\phi(n), \quad (8.1)$$

for the η meson, while it is proportional to

$$\phi^\dagger(0)\gamma_5\gamma_i\phi(0)\phi^\dagger(n)\gamma_5\gamma_i\phi(n), \quad (8.2)$$

for the ω meson. If the zero mode ϕ is an eigenstate of chirality,

$$\phi^\dagger(n)\gamma_5\gamma_i\phi(n)=0. \quad (8.3)$$

Therefore the zero mode does not contribute to G_ω^{DC} . Actually $\gamma_5\phi \approx \pm\phi$. Thus the contribution of zero modes to G_ω^{DC} is small compared with G_η^{DC} . This is the solution for the difference between η and ω .

It was already suggested by Isgur²⁷ and De Rújula, Georgi, and Glashow²⁸ that the existence of the quark-antiquark annihilation diagram for flavor-singlet mesons which corresponds to the G^{DC} is the origin of the η' - π splitting. However, it was not clear why there is no splitting between ρ and ω . One argument which is based on perturbation theory was that the difference between ω and η originates from the fact that two-gluon states can contribute for the pseudoscalar meson, while three-gluon states contribute for the vector meson. However, perturbative theory cannot be applied. Now the reason becomes clear.

B. Flavor-singlet mesons in various channels

In this paper we are mainly interested in the flavor-singlet mesons in the pseudoscalar and vector channels. However, we have also calculated the propagators of the flavor-singlet mesons in the other channels. For the scalar (0^{++}) meson, the G^{DC} is given by

$$\langle \text{Tr}[D^{-1}(0,0)]\text{Tr}[D^{-1}(n,n)] \rangle - \langle \text{Tr}[D^{-1}(0,0)] \rangle^2. \quad (8.4)$$

The first term is nearly independent of n and is identical with the second term up to 4 or 5 digits. Therefore there is a large cancellation between them. This is comparable to the precision of our calculation. Thus, we are unable to obtain meaningful propagators for the flavor-singlet 0^{++} meson. Except for the 0^{++} meson, the second term should be zero and this has been numerically checked. For the 1^{++} and 1^{+-} mesons, it seems that there are no noticeable splittings between the flavor-singlet and -non-singlet mesons, although the data around $t=8$ are not good compared with the 0^{+-} and 1^{--} channels. See Figs. 14 and 15.

The smallness of the G^{DC} for the 1^{+-} meson [$\bar{\psi}(n)\sigma_{ij}\psi(n)$] cannot be understood from the fact that the zero mode is the eigenstate of chirality. However, it can be understood as follows. In the continuum QCD, if we average over the position in space and the orientation in gauge space of an instanton (anti-instanton), we have

$$\phi(x)\bar{\phi}(x) \sim 1 \pm \gamma_5,$$

where ϕ is the zero mode. Therefore

$$\bar{\phi}(x)\sigma_{ij}\phi(x) \sim \text{Tr}[(1 \pm \gamma_5)\sigma_{ij}] = 0.$$

We may expect the same thing in the continuum limit of lattice QCD.

C. Contribution of zero modes to hadron propagators

Let us discuss how zero modes contribute to the propagators of flavor-nonsinglet hadrons. Let us expand the propagators in terms of the eigenfunctions of D for each configuration. Let us consider the contribution of a zero mode ϕ with eigenvalue $1-K/K_c$. For the π meson, the most singular term with coefficient $(1-K/K_c)^{-2}$ is

$$\frac{\phi^\dagger(0)\phi(0)\phi^\dagger(n)\phi(n)}{(\phi^\dagger\gamma_5\phi)^2}. \quad (8.5)$$

This term definitely contributes to the propagator and is the most dominant contribution at $K \sim K_c$. On the other hand, for the ρ meson the most singular term

$$\frac{\phi^\dagger(0)\gamma_5\gamma_i\phi(0)\phi^\dagger(n)\gamma_5\gamma_i\phi(0)}{(\phi^\dagger\gamma_5\phi)^2} \quad (8.6)$$

vanishes if ϕ is the eigenstate of chirality. On a lattice at finite β , zero modes are only approximate eigenstates of chirality and therefore the most singular terms contribute to the ρ propagator but only randomly, because they should not contribute much on the ensemble average. Thus the noise-to-signal ratio at $K \sim K_c^{\text{ensemble}}$ is very large

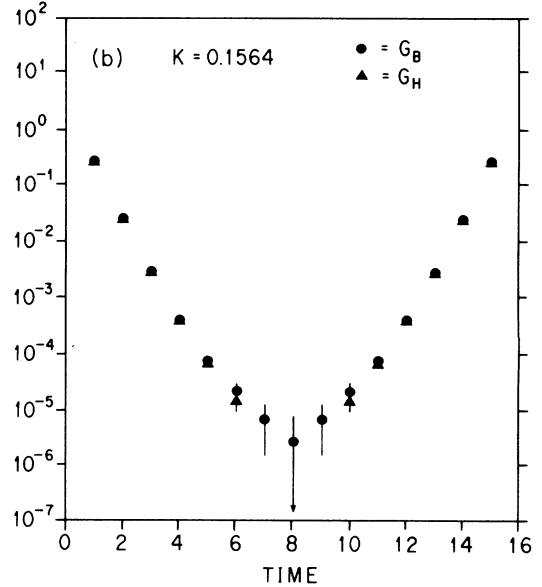
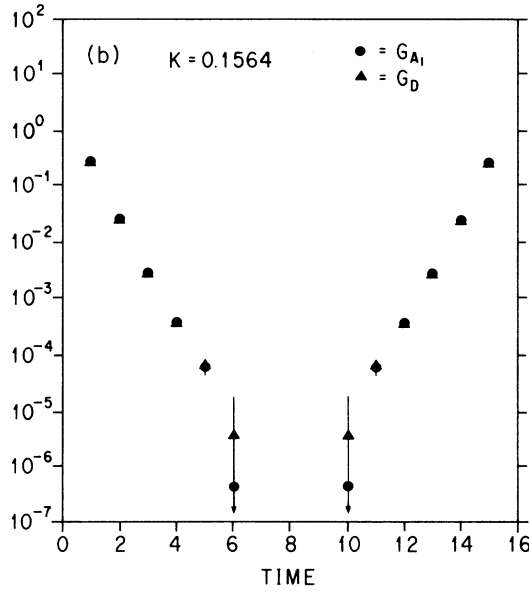
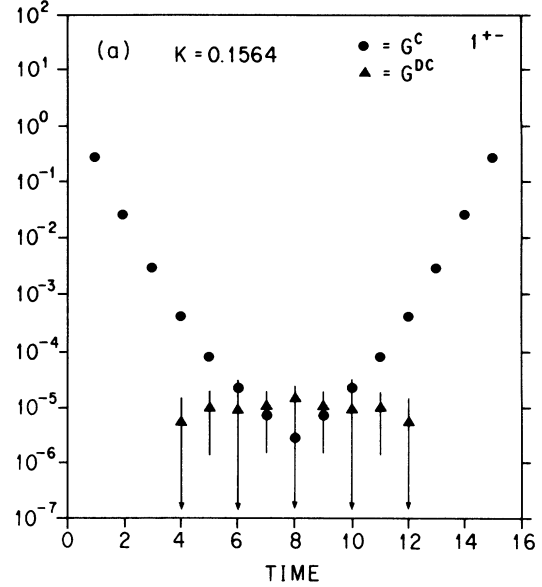
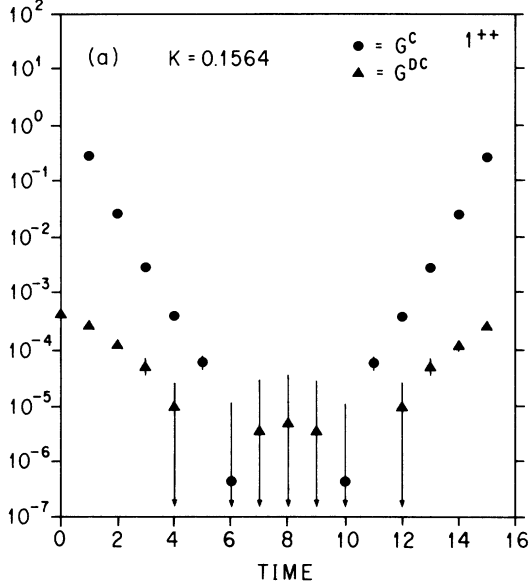


FIG. 14. (a) The $G^C(\mathbf{0},t;0)$ and $G^{DC}(\mathbf{0},t;0)$; (b) the flavor-nonsinglet meson (A_1) and the flavor-singlet meson (D) propagators; for the 1^{++} channel at $K=0.1540$.

FIG. 15. The same as Fig. 14 except for the 1^{+-} channel.

for the ρ propagator compared with the π propagator.

The propagators of baryons are composed of the sum of the product of three quark propagators. After some algebra, we can show that the most singular terms which are composed of three pairs of zero modes do not contribute to the baryon (N and Δ) propagators.

Thus, the most singular terms contribute to the π propagator, while they do not contribute to the ρ , N , and Δ propagators. As $K \rightarrow K_c$, only for the π propagator, one term $\phi^\dagger(0)\phi(0)\phi^\dagger(n)\phi(n)$ dominates. This implies that the π propagator decays slowly, because $\phi^\dagger(n)\phi(n)\phi^\dagger(0)\phi(0)$ is a slowly decaying function of n . Thus the pion mass de-

creases more rapidly compared with the ρ , N , and Δ masses. This will be related with that m_π^2 is a linear function of $1/K$, while m_ρ , m_N , and m_Δ are linear functions of $1/K$, when K is very close to K_c^{ensemble} .

D. Nature of topological excitations

When $\beta \approx \infty$, topologically nontrivial configurations can be identified with instantons as mentioned in Sec. II. Is it possible to identify topologically nontrivial configurations at $\beta=2.4$ with thermal fluctuations around instantons? We believe the answer is “yes” by the follow-

ing analysis. When we plot the $\phi^\dagger(n)\phi(n)$ versus n for the zero mode $\phi(n)$ associated with a topologically nontrivial configuration, it has a peak. (For a $Q=2$ configuration, there are two zero modes each of which has a peak at different points.) See Fig. 16 for a $Q=1$ case; the peak is around $n=(3,6,5,8)$. This behavior is similar to that of the zero mode for an instanton in the continuum QCD, although the behavior of $\phi^\dagger(n)\phi(n)$ versus n for cooled instantons is smoother than that for thermally excited ones.

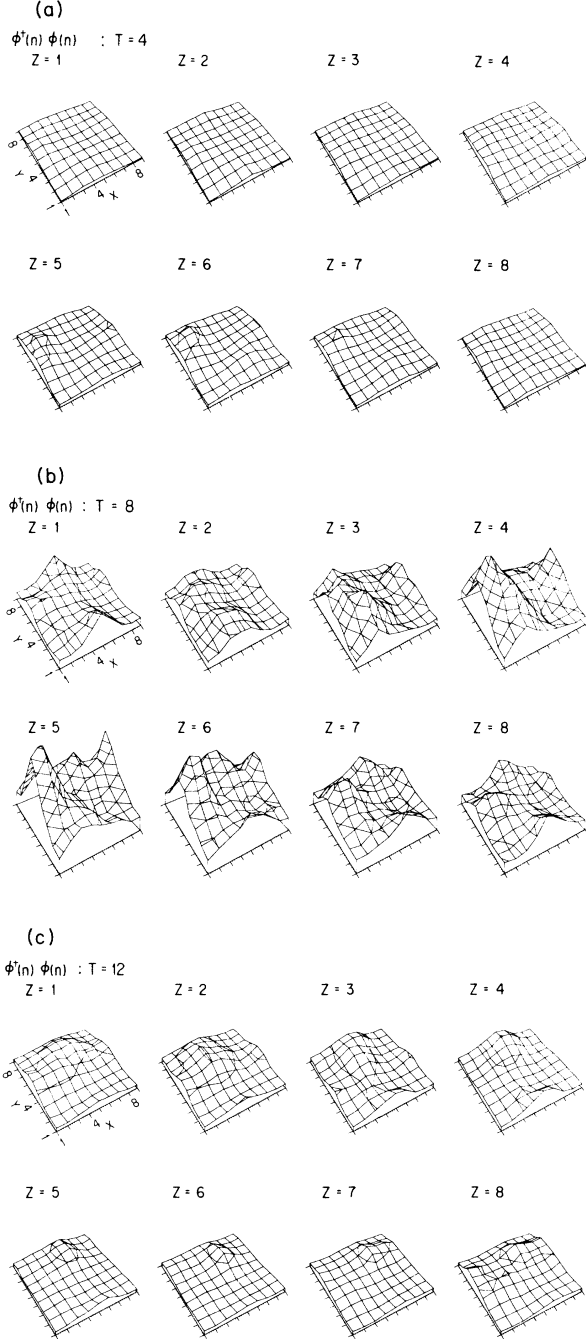


FIG. 16. The scalar density of the zero mode $\phi^\dagger(n)\phi(n)$ vs n for a topologically nontrivial configuration ($Q=1$) at $\beta=2.4$.

(See Fig. 17.) We interpret the position of the peak as the position of a thermally excited instanton. [Note that although $\phi^\dagger(n)\phi(n)$ has a peak at some point $n_0=(n_0, t_0)$, $\phi^\dagger(n)\phi(n)\phi^\dagger(0)\phi(0)$ is a slowly decaying function of n compared with the other propagators as mentioned in Sec. VIII C because (i) when we fix the spatial coordinate \mathbf{n} , the probability that $\mathbf{n}=\mathbf{n}_0$ is negligibly small ($1/8^3$) and (ii) even for the case $\mathbf{n}=\mathbf{n}_0$, when we make the average over the temporal coordinates, the effect of the peak is smoothed down.]

E. Comparison with $1/N$ expanded QCD

Let us now compare our results with the prediction of $1/N$ expanded QCD by Witten³ and Veneziano.⁴ They derived the relation (1.1). In particular, Veneziano in his derivation⁴ has used the relation

$$\begin{aligned} \frac{1}{q^2 + m_S^2} &= \frac{1}{q^2 + m_{NS}^2 + (N_f/N_c)\lambda_\eta^2} \\ &= \frac{1}{q^2 + m_{NS}^2} \left[1 - \frac{1}{q^2 + m_{NS}^2} \frac{N_f}{N_c} \lambda_\eta^2 + \dots \right] \end{aligned} \quad (8.7)$$

and identified each term with a diagram with increasing number of quark loops. (m_S and m_{NS} are the flavor-singlet and -nonsinglet masses, respectively. N_c is the number of color.) If this is valid, the G^C (one loop) and the G^{DC} (two loop) are related by

$$G^C(0, n) = A \int \frac{1}{p^2 + m_{NS}^2} e^{ipn} d^4p \quad (8.8)$$

and

$$G^{DC}(0, n) = A \int \frac{1}{p^2 + m_{NS}^2} \frac{N_f}{N_c} \lambda_\eta^2 \frac{1}{p^2 + m_{NS}^2} e^{ipn} d^4p. \quad (8.9)$$

Here $N_f = N_c = 3$. Denoting m_{NS} simply by m , we obtain, for $n=(0, t)$,

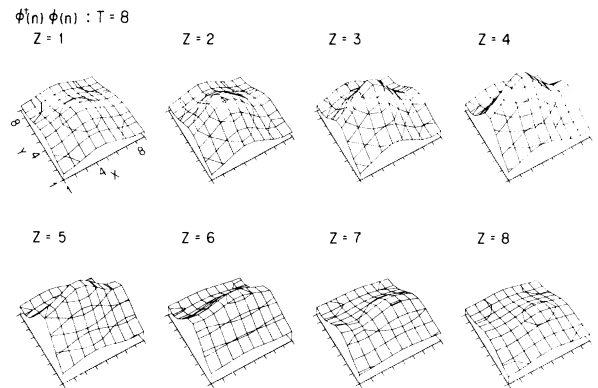


FIG. 17. The same as Fig. 16 except for $\beta \approx \infty$.

$$G^C(0,n) = 4\pi^2 A \frac{m}{t} K_1(mt) \quad (8.10)$$

and

$$G^{DC}(0,n) = 2\pi^2 A \lambda_\eta^2 K_0(mt), \quad (8.11)$$

where K_1 and K_0 are modified Bessel functions. On a lattice the integration ranges over p are limited and therefore the results are slightly different. However, we have checked the difference is not noticeable in the following analyses.

Fitting the $G^C(0,n)$ to

$$4\pi^2 A \left[\frac{m}{t} K_1(mt) + \frac{m}{T-t} K_1(m(T-t)) \right] \quad (8.12)$$

for $6 \leq t \leq 10$, we determine A and m . ($T=16$). Then using the same A and m , we fit the $G^{DC}(0,n)$ to

$$2\pi^2 A \lambda_\eta^2 [K_0(mt) + K_0(m(T-t))], \quad (8.13)$$

at $t=8$ and determine λ_η^2 . We show in Figs. 18 and 19 the results at $K=0.1540$ and $K=0.1564$, respectively. We obtain λ_η^2 , inputting $a^{-1}=1810$ MeV (Ref. 21), as

$$\lambda_\eta^2 = 0.28 \text{ GeV}^2 \quad \text{at } K = 0.154 \quad (8.14)$$

and

$$\lambda_\eta^2 = 0.11 \text{ GeV}^2 \quad \text{at } K = 0.1564. \quad (8.15)$$

On the other hand, in $1/N$ expanded QCD,

$$\lambda_\eta^2 = m_\eta^2 + m_\eta^2 - 2m_K^2 = 0.724 \text{ GeV}^2. \quad (8.16)$$

First we have to check whether the assumption that the one-loop diagram and the two-loop diagram are related by Eqs. (8.8) and (8.9) is satisfied. Because the fitted region for the G^C is already small, it is difficult to judge from the Figure whether G^{DC} is well fitted to the form (8.9). If we could calculate both G^C and G^{DC} on a larger lattice such as $12^3 \times 24$, we think it would be possible to judge the validity of the assumption. Furthermore, because λ_η^2 should be a momentum-independent constant, we can derive a more general relation between G^C and G^{DC} :

$$G^{DC}(n) [= G^{DC}(0,n)] = \lambda_\eta^2 \sum_m G^C(m) G^C(n-m). \quad (8.17)$$

Since we have not calculated the right-hand side, we cannot compare the relation with numerical results. We hope we can do it in the near future. At $K=0.154$ (and also other K 's up to $K=0.154$), the G^{DC} for $t \leq 5$ and $t \geq 11$ is smaller than the fitted curve. If we consider the contribution from excited states, this behavior is inconceivable. Therefore we think the assumption is not valid up to $K=0.154$.

If the assumption (8.9) is valid, $G^C \sim e^{-m_\pi t}/t^{3/2}$ and $G^{DC} \sim e^{-m_\pi t}/t^{1/2}$. On the other hand, our assumption is $G^C \sim e^{-m_\pi t}/t^{3/2}$ and

$$G^{DC} \sim C_2 e^{-m_\pi t}/t^{3/2} + C_3 e^{-m_\eta t}/t^{3/2}.$$

When we compare the results of our assumption (Fig. 9) with the fits to Eq. (8.13) (Figs. 18 and 19), it is difficult to judge which assumption is valid. However, it may be

worthwhile to emphasize that if the assumption (8.13) is valid, the η propagators obtained would behave as

$$[(T/2t)^{3/2} - (T/2t)^{1/2}](e^{-m_\pi t} + e^{-m_\pi(T-t)}), \quad (8.18)$$

where $T=16$. On the other hand, the η propagators obtained decays certainly more rapidly than $e^{-m_\pi t}$ and are consistent with $e^{-m_\eta t}/t^{3/2}$ with $m_\eta \gg m_\pi$ at $K=0.156$ and 0.1564 . We understand this as an indication that our assumption is valid. At any rate, it would be simple to judge if we could have the data on a larger lattice.

Let us now discuss the magnitude of λ_η^2 . Our numerical results differ from the prediction of $1/N$ expanded

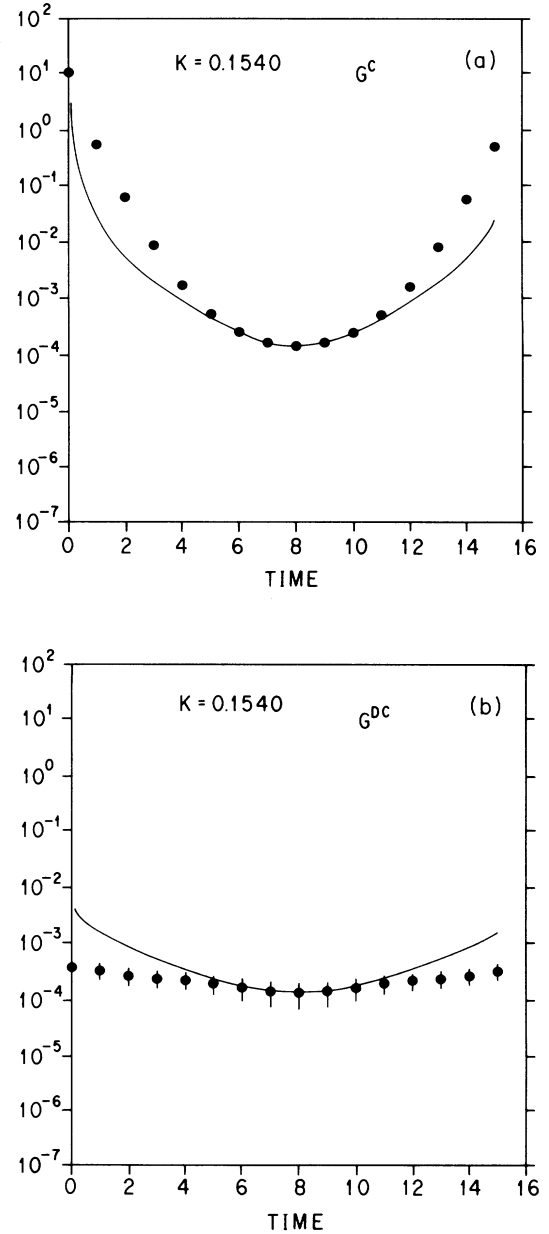


FIG. 18. (a) The G^C together with the fit to Eq. (8.12); (b) the G^{DC} together with the fit to Eq. (8.13); at $K=0.154$.

QCD by a factor 6 at $K=0.1564$. There are several possible reasons for this discrepancy. (i) Our lattice size is not large enough. Therefore the discrepancy is due to finite-size effects. (ii) The basic assumption for G^{DC} , Eq. (8.9), is not valid. (iii) Because the relation is derived in $1/N$ expanded QCD and in the chiral limit, the relation is only an approximate one for $N_c=3$ and for a relatively large strange-quark mass.

Let us finally in this section show the result for the topological susceptibility in our case. We have obtained $\chi_t \simeq [230(13) \text{ MeV}]^4$. This is based on the measurement of the topological charge for 50 configurations after cooling as mentioned in Sec. IV. Our result agrees with other results.⁵ However, we are rather suspicious of the use of the relation (1.1) as a rigorous relation for the real world, because of the reasons given above.

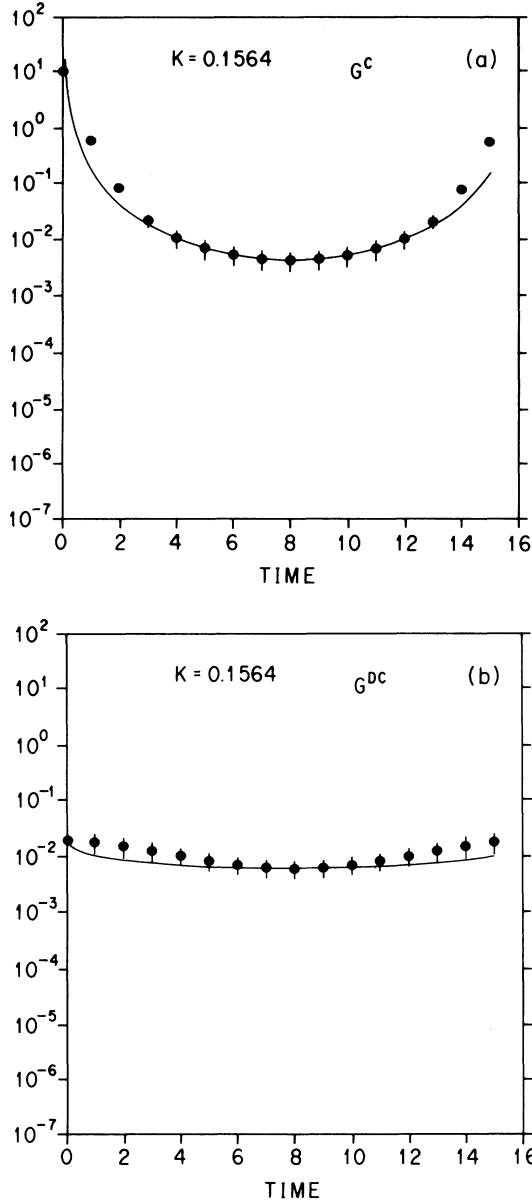


FIG. 19. The same as Fig. 18 except for $K=0.1564$.

F. Comment on Kogut-Susskind fermions

Let us make a comment for Kogut-Susskind fermions. We consider the case of four flavors $[q_\mu^i(n): i=1-4]$ with degenerate mass m , since this is the most natural case for Kogut-Susskind quarks. Let the quark action be $\bar{q}Dq$ with spinor and flavor indices suppressed. When the quark mass equals zero, the quark matrix D anticommutes with²⁹

$$A = \gamma_5 \otimes t_5, \quad (8.19)$$

where γ_5 acts on spinor indices, while t_5 acts on flavor indices:

$$DA = -AD. \quad (8.20)$$

Therefore we can prove that

$$\text{Tr}[D^{-1}(\gamma_5 \otimes I)] = 0, \quad (8.21)$$

because

$$\begin{aligned} \text{Tr}[D^{-1}(\gamma_5 \otimes I)] &= \text{Tr}[D^{-1}(\gamma_5 \otimes I)A^2] \\ &= -\text{Tr}[AD^{-1}(\gamma_5 \otimes I)A] \\ &= -\text{Tr}[D^{-1}(\gamma_5 \otimes I)]. \end{aligned} \quad (8.22)$$

The disconnected part of the propagators of the flavor-singlet pseudoscalar meson for Kogut-Susskind quarks is given by

$$\begin{aligned} G^{DC}(0, n) &= \langle \text{Tr}[D^{-1}(0, 0)(\gamma_5 \otimes I)] \\ &\quad \times \text{Tr}[D^{-1}(n, n)(\gamma_5 \otimes I)] \rangle. \end{aligned} \quad (8.23)$$

Therefore

$$\lim_{V \rightarrow \infty} \lim_{m \rightarrow 0} G^{DC} = 0. \quad (8.24)$$

The only possible way for nonzero G^{DC} is

$$\lim_{m \rightarrow 0} \lim_{V \rightarrow \infty} G^{DC} \neq 0. \quad (8.25)$$

This should be related with the spontaneous breakdown of the symmetry associated by the generator A . Thus even if the U(1) problem would be resolved both for Wilson quarks and Kogut-Susskind quarks, the mechanisms are quite different: For Wilson quarks $\text{Tr}[D^{-1}(n, n)\gamma_5]$ diverges at $K=K_c \sim K_c^{\text{ensemble}}$, while for Kogut-Susskind quarks it is zero when $m=0$ on a finite lattice. This implies the inequivalence of Wilson fermions and Kogut-Susskind fermions even for the case of four flavor with degenerate mass. We have also checked that the minimum (in the magnitude) eigenvalue of D for a topologically nontrivial configuration ($Q=1$) on a 6^4 lattice is of order 0.05, instead of exact zero as in the case for Wilson quarks. (See Ref. 30 for a discussion of the index theorem for Kogut-Susskind fermions.)

Note added in proof. After submitting this paper we noticed that some related works have been done by J. Smit and J. C. Vink. See Ref. 32 and references cited there.

ACKNOWLEDGMENTS

The numerical calculation has been mainly performed with HITAC S810/10 at KEK and partly with HITAC

S810/20 at the University of Tokyo. We would like to thank S. Kabe, T. Kaneko, R. Ogasawara, and other members of Data Handling Division of KEK for their kind arrangement and the members of Theory Division, particularly, H. Sugawara and T. Yukawa for their warm hospitality and strong support for this work. We would like to thank Y. Hara and A. Ukawa for valuable discussions. This work was supported in part by the Grant-in-Aid for Scientific Research of the Ministry of Education (Nos. 61540194 and 61790075). Finally S.I. and T.Y. would like to thank the Iwanami Fujui-kai for financial support.

APPENDIX A: PROOFS OF SEVERAL PROPERTIES FOR THE FERMION MATRIX

We give sketches of the proofs of paragraphs (F1)–(F9) which are given in Sec. III. Paragraphs (P1)–(P9) correspond to (F1)–(F9), respectively.

(P1). The D may be written as

$$D = I + KA, \quad (\text{A1})$$

where I is the identity and K is the hopping parameter. A is K independent. Let

$$A\phi_i = -\frac{1}{\rho_i}\phi_i, \quad (\text{A2})$$

then ρ_i and ϕ_i are K independent. Therefore

$$D\phi_i = (1 - K/\rho_i)\phi_i. \quad (\text{A3})$$

(P5). If

$$D\phi_i = \lambda_i\phi_i, \quad (\text{A4})$$

then

$$\gamma_5 D \gamma_5 \gamma_5 \phi_i = \lambda_i \gamma_5 \phi_i. \quad (\text{A5})$$

Therefore we have

$$D^\dagger \gamma_5 \phi_i = \lambda_i \gamma_5 \phi_i, \quad (\text{A6})$$

which is equivalent to

$$\phi_i^\dagger \gamma_5 D = \lambda_i^* \phi_i^\dagger \gamma_5. \quad (\text{A7})$$

(P2). Let us consider the secular equation for (A7):

$$\det(D - \lambda^* I) = 0. \quad (\text{A8})$$

The eigenvalue λ_i^* is the solution of (A8). This, in turn, implies λ_i^* is also an eigenvalue of D .

(P3). The A defined in (A1) connects only the nearest neighbors. Therefore the sign change of K is equivalent to the alternative sign change of eigenfunctions.

(P4). This can be proved for the free case. For the general case it is a conjecture. For a numerical check see Sec. IV.

(P6). From (A7) we have

$$\phi_i^\dagger \gamma_5 D \phi_j = \lambda_i^* \phi_i^\dagger \gamma_5 \phi_j. \quad (\text{A9})$$

Similarly we have

$$\phi_i^\dagger \gamma_5 D \phi_j = \lambda_j \phi_i^\dagger \gamma_5 \phi_j. \quad (\text{A10})$$

Therefore

$$\phi_i^\dagger \gamma_5 \phi_j = 0 \text{ if } \lambda_i^* \neq \lambda_j. \quad (\text{A11})$$

(P7). Let assume that eigenvalues are not degenerate.

Let

$$P_{ni} = \phi_i(n) / (\bar{\phi}_i^\dagger \gamma_5 \phi_i)^{1/2} \quad (\text{A12})$$

and

$$P_{in}^{-1} = \bar{\phi}_i^\dagger(n) \gamma_5 / (\bar{\phi}_i^\dagger \gamma_5 \phi_i)^{1/2}. \quad (\text{A13})$$

Then the matrices P and P^{-1} satisfy

$$P^{-1}P = I \quad (\text{A14})$$

and

$$P^{-1}DP = \begin{bmatrix} \lambda_1 & & 0 \\ & \lambda_2 & \\ 0 & & \ddots \end{bmatrix}. \quad (\text{A15})$$

Thus we obtain

$$D(n, m) = \sum_i \lambda_i \frac{\phi_i(n) \bar{\phi}_i^\dagger(m) \gamma_5}{\bar{\phi}_i^\dagger \gamma_5 \phi_i}. \quad (\text{A16})$$

Similarly

$$D^{-1}(n, m) = \sum_i \frac{1}{\lambda_i} \frac{\phi_i(n) \bar{\phi}_i^\dagger(m) \gamma_5}{\bar{\phi}_i^\dagger \gamma_5 \phi_i}. \quad (\text{A17})$$

If the matrix D is diagonalizable, we can easily generalize the above proof. The link variables are random numbers. Therefore for the generic case the eigenvalues are nondegenerate and consequently we can assume the spectral representation for D^{-1} .

(P8). Because $(\gamma_5 D)^{-1}$ is a Hermite operator, it is trivial to prove (F8).

(P9). At $K = \rho_i$

$$0 = D\phi_i = \gamma_5 D\phi_i. \quad (\text{A18})$$

Hence for $K \sim \rho_i$, χ_i is written in the form

$$\chi_i = \phi_i + O(\lambda_i). \quad (\text{A19})$$

Substituting Eq. (A19) into Eq. (3.2), we obtain

$$\gamma_5 D(K)[\phi_i + O(\lambda_i)] = \mu_i[\phi_i + O(\lambda_i)]. \quad (\text{A20})$$

Taking the inner product (A20) with $\bar{\phi}_i$, we obtain

$$\lambda_i (\bar{\phi}_i^\dagger \gamma_5 \phi_i) = \mu_i (\bar{\phi}_i^\dagger \phi_i) + O(\lambda_i^2), \quad (\text{A21})$$

because μ_i is of order λ_i .

APPENDIX B: MODIFICATION OF ALGORITHM FOR SOLVING THE QUARK PROPAGATOR

Let us consider the linear equation

$$Dx = b, \quad (\text{B1})$$

for a topologically nontrivial configuration. When K approaches K_c , it becomes difficult to solve the linear Eq. (B1), even if we use the conjugate residual method with an incomplete LU decomposition (ILUCR) which is de-

scribed in Refs. 11 and 31. This is caused by the fact that the zero mode dominates the solution x and the corresponding eigenvalue becomes very small. Therefore we separate the contribution of the zero mode ϕ_0 from the exact solution:

$$x = \frac{\alpha_0}{\lambda_0} \phi_0 + y, \quad (\text{B2})$$

with

$$\alpha_0 = \frac{\phi_0^\dagger \gamma_5 b}{\phi_0^\dagger \gamma_5 \phi_0}. \quad (\text{B3})$$

Thus instead of Eq. (B1) we solve the linear equation for y

$$Dy = b - \alpha_0 \phi_0. \quad (\text{B4})$$

Because the zero mode ϕ_0 does not contribute to the solu-

tion y , we can solve this equation by the standard ILUCR method. We can obtain the solution x from Eq. (B2).

Another way of modification is the modification of the initial approximation of the solution. Let x' be an approximation of the solution and let

$$r = D(x - x') = b - Dx'. \quad (\text{B5})$$

Then we make an improvement of the approximation by

$$x_0 = x' + \frac{r}{\lambda_0}.$$

Note that the zero mode in the solution is exactly given by that in x_0 .

Both modifications work well. The former works slightly better than the latter with respect to the CPU time. On the other hand, the latter is more efficient than the former with respect to the memory size.

¹S. Weinberg, Phys. Rev. D **11**, 3583 (1975).

²G. 't Hooft, Phys. Rev. Lett. **37**, 8 (1976).

³E. Witten, Nucl. Phys. **B156**, 269 (1979).

⁴G. Veneziano, Nucl. Phys. **B159**, 213 (1979).

⁵J. Hoek, M. Teper, and J. Waterhouse, Phys. Lett. **180B**, 112 (1986); M. Göckeler, A. S. Kronfeld, M. L. Laursen, G. Schierholz, and U.-J. Wiese, Report No. DESY-86-107 (unpublished); Y. Arian and P. Woit, Phys. Lett. **183B**, 341 (1987).

⁶K. G. Wilson, Phys. Rev. D **14**, 2445 (1974).

⁷S. Itoh, Y. Iwasaki, and T. Yoshié, Phys. Lett. **184B**, 375 (1987).

⁸H. Hamber and G. Parisi, Phys. Rev. D **27**, 208 (1983); M. Fukugita, T. Kaneko, and A. Ukawa, Phys. Lett. **145B**, 93 (1984).

⁹K. G. Wilson, in *New Phenomena in Subnuclear Physics*, Erice, 1975, edited by A. Zichichi (Plenum, New York, 1977).

¹⁰L. Susskind, Phys. Rev. D **16**, 3931 (1977).

¹¹S. Itoh, Y. Iwasaki, Y. Oyanagi, and T. Yoshié, Nucl. Phys. **B274**, 33 (1986).

¹²M. Bochicchio, L. Maiani, G. Martinelli, G. Rossi, and M. Testa, Nucl. Phys. **B262**, 331 (1985).

¹³Y. Iwasaki, Nucl. Phys. **B258**, 141 (1985); Report No. UTHEP-118 (unpublished).

¹⁴Y. Iwasaki and T. Yoshié, Phys. Lett. **131B**, 159 (1983).

¹⁵S. Itoh, Y. Iwasaki, and T. Yoshié, Phys. Lett. **147B**, 141 (1984).

¹⁶M. Atiyah and I. Singer, Ann. Math. **87**, 484 (1968).

¹⁷M. Lüscher, Commun. Math. Phys. **85**, 39 (1982).

¹⁸J. Polonyi, Phys. Rev. D **29**, 716 (1984).

¹⁹P. Woit, Phys. Rev. Lett. **51**, 638 (1983).

²⁰G. Parisi and F. Rapuano, Phys. Lett. **152B**, 218 (1985).

²¹S. Itoh, Y. Iwasaki, and T. Yoshié, Phys. Lett. **183B**, 351 (1987).

²²F. Karsh, E. Seiler, and I. O. Stamatescu, Nucl. Phys. **B271**, 349 (1986).

²³S. Itoh, Y. Iwasaki, and T. Yoshié, Phys. Lett. **167B**, 443 (1986).

²⁴S. Itoh, Y. Iwasaki, and T. Yoshié, Phys. Rev. D **33**, 1806 (1986).

²⁵Y. Iwasaki, Report No. UTHEP-164 (unpublished).

²⁶J. L. Rosner, in *Proceedings of the 1985 International Symposium on Lepton and Photon Interactions at High Energies*, Kyoto, Japan, 1985, edited by M. Konuma and K. Takahashi (Research Institute for Fundamental Physics, Kyoto University, Kyoto, 1986).

²⁷N. Isgur, Phys. Rev. D **13**, 122 (1976).

²⁸A. De Rújula, H. Georgi, and S. L. Glashow, Phys. Rev. D **12**, 47 (1975).

²⁹H. Kluberg, A. Morel, O. Napoly, and B. Petersson, Nucl. Phys. **B220** [FS8], 447 (1983).

³⁰E.-M. Ilgenfritz, M. L. Laursen, M. Müller-Preussker, G. Schierholz, and H. Schiller, Nucl. Phys. **B268**, 693 (1986); I. Barbour and M. Teper, Phys. Lett. **175B**, 445 (1986).

³¹Y. Oyanagi, Report No. ISE-TR-86-57, 1986 (unpublished).

³²J. Smit and J. C. Vink, Report No. ITFA-86-24, 1986 (unpublished).